

**Multiphase Flow in Naturally Fractured Reservoirs: Comparison of  
Matrix-Fracture Shape Factor and Transfer Function**

by

Lai Kok Soon

Dissertation submitted in partial fulfillment of

the requirements for the

Bachelor of Engineering (Hons)

(Mechanical Engineering)

MAY 2012

Universiti Teknologi PETRONAS

Bandar Seri Iskandar

31750 Tronoh

Perak Darul Ridzuan

# **CERTIFICATION OF APPROVAL**

Comparison of Matrix-Fracture Transfer Function and Shape Factor

by

Lai Kok Soon

A project dissertation submitted to the

Mechanical Engineering Programme

Universiti Teknologi PETRONAS

in partial fulfillment of the requirement for the

BACHELOR OF ENGINEERING (Hons)

(MECHANICAL ENGINEERING)

Approved by,

---

(Dr. William Pao King Soon)

UNIVERSITI TEKNOLOGI PETRONAS

TRONOH, PERAK

MAY 2012

## **CERTIFICATION OF ORIGINALITY**

This is to certify that I am responsible for the work submitted in this project, that the original work is my own except as specified in the references and acknowledgements, and that the original work contained herein have not been undertaken or done by unspecified sources or persons.

---

(Lai Kok Soon)

## ABSTRACT

The first part is the comparison of shape factor by using dimensionless terms and second part is comparison of transfer function. In the first part, the influence of different shape factors is represented in dimensionless pressure and dimensionless time. A new correlation is derived to relate these dimensionless terms with matrix-fracture transfer rate. This comparison summarizes that the effect of shape factors can be generalized by defining the rate of change of matrix-fracture transfer. In the second part, comparison of transfer function is done by using a reservoir test problems from Sixth SPE Comparison Project. Comparison of transfer function showed that direct generalization from single phase to multiphase is insufficient for modeling matrix-fracture transfer rate. It also demonstrates the imbibition terms should be considered in transfer function.

## **ACKNOWLEDGEMENT**

First and foremost, I would like to thank my supervisor Dr. William Pao for his support, encouragement, and guidance. It is evident that this work would not have been possible without his patronage. I would also like to express my gratitude to Dr. Fakhruddin Bin Mohd Hashim and Ms. Chin Yee Sing for their valuable feedback. I also wish to thank the rest of the Mechanical Engineering Department for their support and contributions to my academic achievements.

## TABLE OF CONTENTS

CERTIFICATION OF APPROVAL.....	1
ABSTRACT .....	3
ACKNOWLEDGEMENT.....	4
CHAPTER 1 : INTRODUCTION.....	9
1.1 Background.....	9
1.2Theories & Concepts Review .....	10
1.3Objectives .....	10
1.4Scope of Work.....	10
CHAPTER 2 : LITERATURE REVIEW.....	12
2.1 Double Porosity Models .....	12
2.2 Early Researches .....	12
2.3 Recent Researches .....	17
2.4 Concluding Remarks .....	20
CHAPTER 3 : METHODOLOGY.....	22
3.1 Overview of Research Methodology.....	22
3.2 Research Flow Chart .....	23
3.3 Program flow chart of NFR simulator.....	25
3.4 Brief Descriptions of the Selected NFR Simulator Software .....	28
3.5 Gantt Chart and Milestone.....	30
3.5.1 Final Year Project 1 .....	30
3.5.2 Final Year Project 2 .....	31
3.6 Selection of Base Cases.....	32
3.6.1 Comparison of constant shape factor .....	32
3.6.2 Comparison of transfer function .....	32
3.6.3 Reservoir Properties.....	33
3.7 Derivation of Kazemi Shape Factor for Various Geometries. ....	36
3.7.1 Kazemi's cylinder shape factor.....	36
3.7.2 Kazemi's sphere shape factor .....	36
3.7.3 Kazemi's tetrahedron shape factor.....	37
CHAPTER 4 : VALIDATIONS OF NFR SIMULATOR SOFTWARE.....	39
4.1 Verifications of the Selected NFR Simulator .....	39

CHAPTER 5 : RESULTS & DISCUSSION.....	41
5.1 Comparison of Shape Factor .....	41
5.1.1 Single Set of Fractures .....	42
5.1.2 Double set of fractures & Triple set of fractures .....	43
5.1.3 Different geometries .....	44
5.3 Comparison of time dependent transfer functions.....	46
5.3.1 Verifications & comparison of results .....	47
CHAPTER 6 : CONCLUSION & RECOMMENDATION .....	49
6.1 Conclusion.....	49
6.2 Recommendations .....	49
NOMENCLATURE .....	50
REFERENCES .....	51
APPENDIX .....	54
A.1. Visualization of reservoir problem (shape factor comparison) .....	54
A.2. Derivation of correlation of transfer rate and $P_d / t_d$ .....	55
A.3. Water saturation profile in reservoir blocks using various transfer functions .....	56
A.3.1 Simulation using Warren & Root (1963) transfer function .....	57
A.3.2 Simulation using Sarma & Aziz (2006) transfer function .....	59
A.3.3 Simulation using Rangel-German & Kovsky (2005) transfer function .....	61

## LIST OF FIGURES

Figure 1: Idealization of the heterogeneous porous medium (Warren and Root, 1963) .....	12
Figure 2: Schematic of an elemental reservoir volume in a naturally fractured reservoir and idealization of flow and elemental reservoir volumes containing matrix blocks in a naturally fractured reservoir. (Kazemi et al., 1976).....	13
Figure 3: Discretization of a 2D fracture network – fracture cells and matrix blocks (Sarda et al., 2002).....	18
Figure 4: Research Flow Chart.....	24
Figure 5: NFR Simulator Program Flow Chart, module 1 to 4. ....	25
Figure 6: NFR Simulator Program Flow Chart, module 5 to 13. ....	26
Figure 7: NFR Simulator Program Flow Chart, module 14 to 22. ....	27
Figure 8: (a) A matrix block with 3 set of fractures (b) crosssection of matrix showing the flow mechanism .....	28
Figure 9: (a) A matrix block with 2 set of fractures (b) crosssection of matrix showing the flow mechanism .....	29
Figure 10: (a) A matrix block with 1 set of fractures (b) crosssection of matrix showing the flow mechanism .....	29
Figure 11: Simulation result of basic double porosity NFR simulator. The transfer function in the simulator is from Warren & Root (1963).....	40
Figure 12: Single set of fractures: Dimensionless pressure vs dimensionless time ..	42
Figure 13: Double set of fractures: Dimensionless pressure vs dimensionless time.	43
Figure 14: Triple set of fractures: Dimensionless pressure vs dimensionless time ..	44
Figure 15: Various geometries: Dimensionless pressure vs dimensionless time.....	45
Figure 16: Simulation of 15x1x1 blocks with water injection & oil production with different researcher’s shape factor (single set of fractures). The problem is taken from BOAST-NFR manual. BOAST-NFR uses Lim & Aziz (1995) shape factor...	46
Figure 17: Simulation result of double porosity NFR simulator with 3 different transfer functions. ....	48
Figure A1: One of the simulations runs using Kazemi’s shape factor for tetrahedron. .....	54



Figure A2: Water saturation in matrix blocks at time=486.4days.....	57
Figure A3: Water saturation in matrix blocks at time=2485.6days.....	57
Figure A4: Water saturation in fractures at time=486.4days .....	58
Figure A5: Water saturation in fractures at time=2485.6days .....	58
Figure A6: Water saturation in matrix blocks at time=486.4days.....	59
Figure A7: Water saturation in matrix blocks at time=2485.6days.....	59
Figure A8: Water saturation in fractures at time=486.4days .....	60
Figure A9: Water saturation in fractures at time=2485.6days .....	60
Figure A10: Water saturation in matrix blocks at time=486.4days.....	61
Figure A11: Water saturation in matrix blocks at time=2485.6days.....	61
Figure A12: Water saturation in fractures at time=486.4days .....	62
Figure A13: Water saturation in fractures at time=2485.6days .....	62

## **LIST OF TABLES**

Table 1: Overview of Shape Factors in the Literature .....	21
Table 2: Summary of Research Works and Methodologies .....	23
Table 3: Final Year Project 1 Gantt chart.....	30
Table 4: Final Year Project 2 Gantt chart.....	31
Table 5: Basic data for depletion run. ....	32
Table 6: Basic data for water-injection case* .....	33
Table 7: Layer data* .....	33
Table 8: Wells information* .....	33
Table 9: Basic Reservoir Properties** .....	34
Table 10: Density of oil, water, and gas at standard condition** .....	34
Table 11: Relative permeability data** .....	34
Table 12: Saturated oil properties** .....	35
Table 13: Water properties** .....	35
Table 14: Gas properties** .....	35
Table 15: Summary of different geometries shape factors.....	38

# CHAPTER 1

## INTRODUCTION

### 1.1 Background

According to Zhang et al. (2010), naturally fractured and vuggy reservoirs are commonly found around the world and contribute substantially to the global hydrocarbon production. Naturally fractured reservoirs have several important features: (a) they form important component parts of the oil reserves, (b) difficulties in field development due to the presence of fractures and vugginess, (c) strongly heterogeneous due to intense fracturing, and (d) require water flooding in later development stage. The naturally fractured reservoir is a complex system with irregular fractures network, vugs, and matrix blocks. It can also be defined as a reservoir having a connected fractures network which has significant higher permeability than matrix. This implies that production of hydrocarbons is highly dependent on the fractures network. With a better understanding of naturally fractured reservoirs, engineers can maximize the reservoir recovery. However, understanding the behaviors of naturally fractured reservoirs are difficult because of the complexity and numerical challenges in solving a large set of coupled partial differential equations.

The earliest researchers that started to model naturally fractured reservoirs were Warren and Root (1963). They have used the concept of double porosity to model naturally fractured reservoirs. In the model, matrix is mainly the storage medium while fractures provide the fluid flow path. Since then, different models were developed as variations of the Warren and Root (1963) concept of double porosity. Ultimately, all models were developed to increase the accuracy in estimating the well performances of naturally fractured reservoirs. This research is to compare different models of naturally fractured reservoir for multiphase flow focusing on the leakage formulation from matrix to fracture flow path.

## 1.2 Theories & Concepts Review

Naturally fractured reservoir can be modeled by having 2 separate partial differential equations to define matrix and fracture flow. Matrix usually have low permeability and high storativity, while fractures have high permeability but low storativity. This suggest that matrix function as a main source of hydrocarbons while, fractures become the flow path of hydrocarbon production. For this reason, interaction between matrix and fractures must be considered. Interaction between matrix and fractures can be described by using a transfer function. Matrix-fractures transfer function was first introduced by Warren and Root (1963) and it is given as

$$q = \sigma \frac{kV}{\mu} (p_m - p_f) \quad (1.1)$$

Eq. (1.1) showed that the matrix-fracture transfer function which requires leakage coefficient  $\sigma$  that governs the flow rate between matrix and fracture. This leakage coefficient  $\sigma$  is commonly known as shape factor.

## 1.3 Objectives

Primary objective of this research is to **compare different models** of **naturally fractured reservoir** for **multiphase flow** focusing on the **leakage formulation** from matrix to fracture flow path.

## 1.4 Scope of Work

The scope of this research includes:

- (a) Selects an appropriate base case model.
- (b) Analyze the computation modules in a dual porosity naturally fractured reservoirs (NFR) simulator.
- (b) Study the derivation of different leakage terms for matrix and fracture
- (c) Implements different leakage coefficients into NFR simulator and compares the results.

(d) Implements different transfer functions into NFR simulator and compares the results.

(d) Generate appropriate NFR simulator output for visualization.

## CHAPTER 2

### LITERATURE REVIEW

This chapter gives an exposition of selected double porosity models and shape factors in simulating naturally fractured reservoirs.

#### 2.1 Double Porosity Models

In double porosity model, two separate expressions were used to describe the flow in fractures and matrix. Barenblatt et al. (1960) were the first to introduce the concept of double porosity. However, Warren and Root (1963) were the one that uses the double porosity concept to characterize naturally fractured reservoirs.

#### 2.2 Early Researches

Warren and Root (1963) used assumption of pseudosteady flow and simplified naturally fractured reservoir into blocks of matrix and fractures set that looks like sugar cubes. Each cube is known as matrix that contained in within a systematic array of identical and rectangular parallelepipeds. Matrix is assumed to be homogenous and isotropic. All the fractures are continuous and may have different spacing and width to simulate certain degree of anisotropy. Flows can occur in fractures, between matrix and fractures but not through the matrix. Figure 1 shows the idealization of reservoir block as sugar cubes model.

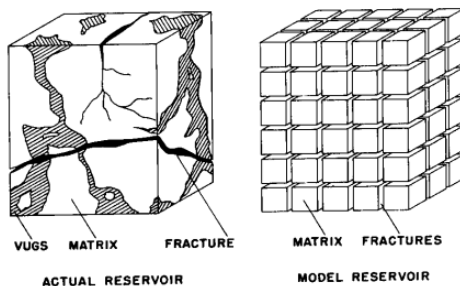


Figure 1: Idealization of the heterogeneous porous medium (Warren and Root, 1963)

As previously mentioned in Eq.(1.1), Warren and Root (1963) introduced an expression that require shape factor. Warren and Root (1963) defined shape factor as

$$\sigma = \frac{4n(n+2)}{l^2} \quad (2.1)$$

where  $n$  refers to the number fractures set =1,2,3 and  $l$  refers to

$$n=3; l = \frac{3L_x L_y L_z}{L_x L_y + L_x L_z + L_y L_z} \quad (2.2)$$

$$n=2; l = \frac{2L_x L_y}{L_x + L_y} \quad (2.3)$$

$$n=1; l = L_x \quad (2.4)$$

Later, Kazemi et al. (1976) produced a three-dimensional numerical simulator for two-phase flow of water and oil in naturally fractured reservoirs. Their model accounts for relative fluid mobility, gravity forces, imbibition, and variation in reservoir properties. Subsequently, this model becomes one of the main reference lines for other researchers to compare results (Coats, 1989; Dutra and Aziz, 1992; Sarma and Aziz, 2006; Lu et al. 2008). Figure 2 shows the concepts used by Kazemi et al. (1976).

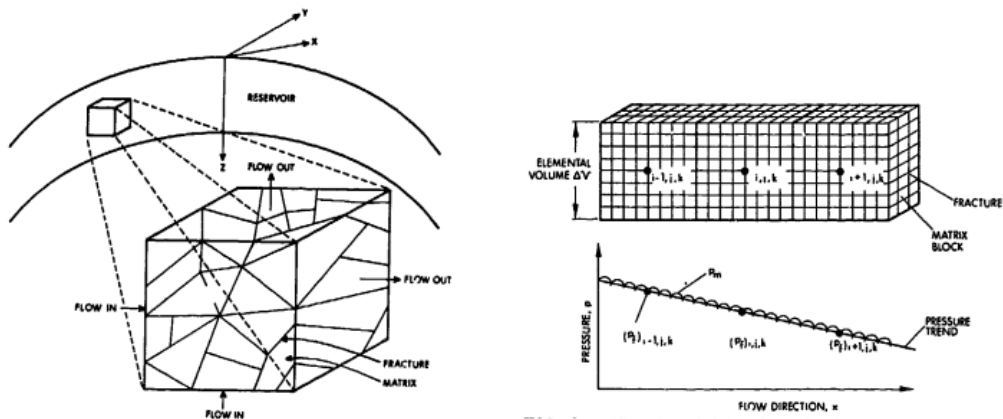


Figure 2: Schematic of an elemental reservoir volume in a naturally fractured reservoir and idealization of flow and elemental reservoir volumes containing matrix blocks in a naturally fractured reservoir. (Kazemi et al., 1976)

In additions, Kazemi et al. (1976) developed new shape factors for their simulator using finite difference method. Their shape factors for rectangular geometry are:

$$1 \text{ set of fractures; } \sigma = 4 \left( \frac{1}{L_x^2} \right) \quad (2.5)$$

$$2 \text{ set of fractures; } \sigma = 4 \left( \frac{1}{L_x^2} + \frac{1}{L_y^2} \right) \quad (2.6)$$

$$3 \text{ set of fractures; } \sigma = 4 \left( \frac{1}{L_x^2} + \frac{1}{L_y^2} + \frac{1}{L_z^2} \right) \quad (2.7)$$

In following years, Kazemi & Gilman (1992) introduced a generalized shape factor Eq. (2.8) and shape factor for cylinder shape Eq. (2.9). Though, the full derivation of generalized shape factor Eq. (2.8) was only shown by Heinemann and Mittermeir (2011) in recent years.

$$\sigma_{general} = \frac{1}{V_m} \sum_s \frac{A_m}{d_m} \quad (2.8)$$

$$\sigma_{cylinder} = \frac{4}{h^2} + \frac{2}{r^2} \quad (2.9)$$

Coats (1989) developed a model that simulates unsteady-state three dimensional and three phase flow in heterogeneous reservoirs. Coats also came up with new shape factors for his model. Coats' shape factors for rectangular geometry are:

$$1 \text{ set of fractures; } \sigma = 8 \left( \frac{1}{L_x^2} \right) \quad (2.10)$$

$$2 \text{ set of fractures; } \sigma = 8 \left( \frac{1}{L_x^2} + \frac{1}{L_y^2} \right) \quad (2.11)$$

$$3 \text{ set of fractures; } \sigma = 8 \left( \frac{1}{L_x^2} + \frac{1}{L_y^2} + \frac{1}{L_z^2} \right) \quad (2.12)$$

The value of the shape factors are doubled of the Kazemi et al. (1976) shape factors. However, the method to arrive at this shape factors is through Fourier finite sine transform and integration. Fourier transformation was also used by Chang (1993) and Lim & Aziz (1995) to arrive at another shape factors different from Coats (1989). Coats' work became the main references for Chang (1993) and Lim & Aziz (1995). Both Chang (1993) and Lim & Aziz (1995) continued Coats' work but with different boundary conditions. By using pressure boundary conditions, Chang (1993) and Lim & Aziz (1995) arrived at same shape factors for rectangular geometry. Their shape factors are:

$$1 \text{ set of fractures; } \sigma = \pi^2 \left( \frac{1}{L_x^2} \right) \quad (2.13)$$

$$2 \text{ set of fractures; } \sigma = \pi^2 \left( \frac{1}{L_x^2} + \frac{1}{L_y^2} \right) \quad (2.14)$$

$$3 \text{ set of fractures; } \sigma = \pi^2 \left( \frac{1}{L_x^2} + \frac{1}{L_y^2} + \frac{1}{L_z^2} \right) \quad (2.15)$$

Lim & Aziz (1995) added that the total amount of mass entered a system at time  $t$ ,  $M_t$  and corresponding mass after infinite time,  $M_\infty$  can be expressed as:

$$\frac{M_t}{M_\infty} = \frac{\bar{p}_m - p_i}{p_f - p_i} = \frac{\bar{p}_m - p_i}{p_f - p_i} \quad (2.16)$$

Eq. (2.17) –Eq. (2.20) are the analytical solutions given by Lim & Aziz for single phase matrix-fracture transfer. The solutions can be differentiated to obtain respective shape factors.

$$1 \text{ set of fractures; } \frac{\bar{p}_m - p_i}{p_f - p_i} = 1 - 0.81 \exp \left[ \frac{-\pi^2 kt}{\phi \mu c_i L^2} \right] \quad (2.17)$$



$$2 \text{ set of fractures (circle); } \frac{\bar{p}_m - p_i}{p_f - p_i} = 1 - 0.69 \exp \left[ \frac{-5.78kt}{\phi\mu c_i R^2} \right] \quad (2.18)$$

$$3 \text{ set of fractures (sphere); } \frac{\bar{p}_m - p_i}{p_f - p_i} = 1 - 0.61 \exp \left[ \frac{-\pi^2 kt}{\phi\mu c_i R^2} \right] \quad (2.19)$$

3 set of fractures (rectangular);

$$\frac{\bar{p}_m - p_i}{p_f - p_i} = 1 - \left( \frac{8}{\pi^2} \right)^3 \exp \left[ \frac{-\pi^2 t \left( \frac{k_x}{L_x^2} + \frac{k_y}{L_y^2} + \frac{k_z}{L_z^2} \right)}{\phi\mu c_i} \right] \quad (2.20)$$

Eq. (2.18) and Eq. (2.19) can be further differentiate to obtain shape factors for cylinder 2D and sphere 3D which are  $\sigma_{cylinder} = \frac{5.78}{r^2}$  and  $\sigma_{sphere} = \frac{\pi^2}{r^2}$ .

Meanwhile, Chang (1993) has derived another shape factors using constant flow rate boundary conditions which are:

$$1 \text{ set of fractures; } \sigma = 12 \left( \frac{1}{L_x^2} \right) \quad (2.21)$$

$$2 \text{ set of fractures; } \sigma = 12 \left( \frac{1}{L_x^2} + \frac{1}{L_y^2} \right) \quad (2.22)$$

$$3 \text{ set of fractures; } \sigma = 12 \left( \frac{1}{L_x^2} + \frac{1}{L_y^2} + \frac{1}{L_z^2} \right) \quad (2.23)$$

On the other hands, Quintard & Whitaker (1995) used assumption of infinite permeability in the fracture to set the boundary value problem for double porosity flow. By solving using Fourier series for rectangular geometry, they reached conclusion of shape factors which are:

$$1 \text{ set of fractures } \sigma = 12 \left( \frac{1}{L_x^2} \right) \quad (2.24)$$

$$2 \text{ set of fractures } \sigma = 14.22 \left( \frac{1}{L_x^2} + \frac{1}{L_y^2} \right) \quad (2.25)$$

$$3 \text{ set of fractures } \sigma = 16.54 \left( \frac{1}{L_x^2} + \frac{1}{L_y^2} + \frac{1}{L_z^2} \right) \quad (2.26)$$

### 2.3 Recent Researches

Recent researches focus more on the time dependent shape factors rather than constant shape factors that were discussed in earlier literature review. Penuela et al. (2002) derived time dependent flow correction factor and incorporated it in the BOAST-NFR. Their time dependent flow correction factor is a function of water relative permeability. They mentioned that the correction factor converges to the constant shape factors as given by Eq. (2.27).

$$\lim_{t \rightarrow \infty} \frac{4\sigma_c(t)}{L^2} = \sigma \quad (2.27)$$

$$\sigma_c = f_{kn} \left( \frac{1}{t_d} + \frac{1 \times 10^{-5}}{t_d^2} \right)^{1/2} \quad t_d < t_d^* \quad (2.28)$$

$$\sigma_c = 2.47 \left( 1 + \frac{473.04}{t_d^{3/4}} \right) \quad t_d \geq t_d^* \quad (2.29)$$

$$f_{kn} = (1.67 - 0.167n_o) \left( 749k_{rw}^{*2} - 1524k_{rw}^* + 1275 \right) \quad (2.30)$$

Expression for time dependent flow correction factors were given in Eq. (2.28) and Eq. (2.29). By using regression analysis, Penuela et al. (2002) obtained the correlations as in Eq. (2.30) and categorized the flow correction factor into 2 flow periods. It can be concluded that this time dependent correction factors are relatively accurate and easy to be implemented in dual porosity models.

Sarda et al. (2002) conducted studies on discrete fractures network in simulating fractured reservoirs. Figure 3 shows the approaches used by them in discretizing a

2D fracture network. In their research, they came up with shape factors constant which was in between Quintard & Whitaker (1995) and Lim & Aziz (1995). The approach used by Sarda et al. (2002) is a numerical method but it is not explained in details. For the parallelepiped fracture network, their shape factors are given as  $8/L^2$  for a 1D transfer,  $24/L^2$  for a 2D transfer and  $48/L^2$  for a 3D transfer.

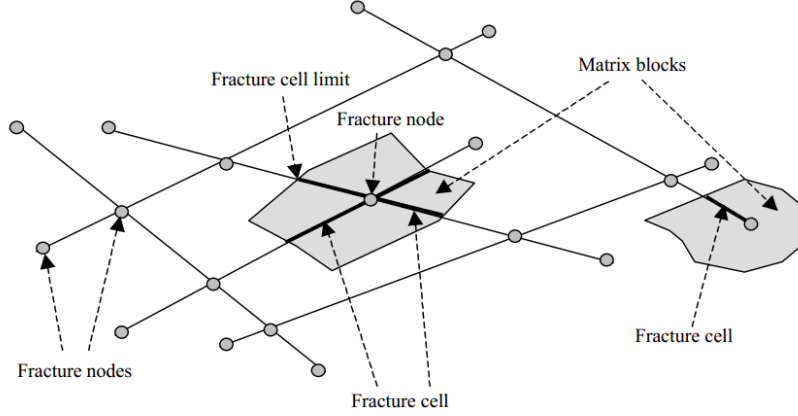


Figure 3: Discretization of a 2D fracture network – fracture cells and matrix blocks (Sarda et al., 2002)

Rangel-German and Kovscek (2005) performed various experiment together with analytical calculations and numerical reservoir simulation to examine the imbibition of water. They stated that transfer function for pressure and water capillary action under immiscible conditions was:

$$q_w = \sigma_p V \bar{K} \frac{k_{rw}}{\mu_w} (\bar{p}_{wm} - p_{wf}) - \sigma_s V D_h (S_{wmax} - \bar{S}_{wm}) \quad (2.31)$$

$$\sigma_s(t) = \frac{A(t)}{VL^*(t)}; \quad \sigma_s = \sigma^* \left( \frac{t_d}{t_d^*} \right)^{-m} \quad \text{for} \quad t_d < t_d^* \quad (2.32)$$

$$\sigma_s = \sigma^* \quad \text{for} \quad t_d \geq t_d^* \quad (2.33)$$

Here,  $m$  is a function of flow rate and fracture aperture. It can be observed that  $\sigma_s$  converges to constant shape factor.

Sarma and Aziz (2006) derived an analytical time dependent shape factor Eq. (2.34) that account for both transient and pseudosteady-state flow. Despite that, they did not incorporate it in their new transfer function. Instead, their new transfer function has two different shape factors. The transfer function Eq. (2.36) has the similar form as Rangel-German and Kavscek (2005) Eq. (2.33).

$$\sigma = -\frac{1}{D(\bar{p}_m - p_f)} \frac{\partial \bar{p}_m}{\partial t} \quad (2.34)$$

$$\bar{p}_m(t) = \frac{\sum_{i=1}^n V_i p_i(t)}{\sum_{i=1}^n V_i} \quad (2.35)$$

$$Q_{wvf} = V \rho_w \lambda_w \sigma_{PD} (\bar{p}_w - p_{wf}) - V \phi \rho_w \sigma_{SD} (\bar{S}_w - S_{wi}) \quad (2.36)$$

$$\sigma_{PD} = \frac{\pi^2}{L^2} \quad (2.37)$$

$$\sigma_{SD} = \left( \frac{8}{\pi^2} + 1 \right) \frac{D(t)}{2 \int_0^t D(\tau) d\tau} = bt^{-1} \quad (2.38)$$

Lu et al. (2008) used a different approach to derive a general transfer function for multiphase flow in fractured reservoirs. They considered transfer in matrix and fracture to be a combination of physical influences from fluid expansion, diffusion, imbibition, and gravity drainage. They categorized physical influences into 3 terms which are fluid expansion, diffusion, and fluid displacement. Fluid displacement refers to the horizontal and vertical displacement due to capillary imbibition and gravity drainage. Although different approaches were used, shape factor is still required for the general transfer function.

## 2.4 Concluding Remarks

a) Throughout the past five decades, there have been many continuous researches in modeling naturally fractured reservoirs. The growing interest in modeling naturally fractured reservoirs have led to the SPE 6<sup>th</sup> Comparative Solution Project: Dual Porosity Simulators, 1990. Firoozabadi & Thomas (1990) has selected 2 problems for the comparative projects. The problems were a depletion simulation of single block and more complicated blocks ( $n_x = 10, n_y = 1, n_z = 5$ ) with gas-injection and water-injection cases. The comparative project were participated by nine different companies. The companies are Chevron Oil Field Research Co., Computer Modelling Group (CMG), Dancomp A/S, Exploration Consultant Ltd. (ECL), Franlab, Japan Oil Engineering Co. (JOE), Marathon Oil Co., Phillips Petroleum Co., Simulation and Modelling Consultancy Ltd. (SMC), and Scientific Software-Intercomp (SSI). The results of the comparative project are very useful for validation purposes of any naturally fractured reservoirs simulator.

b) Shape factor was one of the crucial parameters in double porosity model. There were many variations of shape factors, from constant to time dependent shape factor. Recent years, focuses are shifted onto time dependent shape factor because of the need to have higher accuracy in simulating naturally fractured reservoirs. Table 1 summarizes the all the constant shape factors in the literature.

c) Penuela et al. (2002), Rangel-German & Kovsky (2005), and Sarma & Aziz (2006) have conducted research on time-dependency of transfer functions. It can be concluded that imbibition of water must be considered especially when involving water injection cases. Time-dependent transfer function is concluded to be a function of water properties.

Author	1D	2D	3D
Warren & Root (1963)	$\frac{12}{L_x^2}$	$\frac{32}{l^*}$	$\frac{60}{l^*}$
Kazemi et al. (1976)	$4\left(\frac{1}{L_x^2}\right)$	$4\left(\frac{1}{L_x^2} + \frac{1}{L_y^2}\right)$	$4\left(\frac{1}{L_x^2} + \frac{1}{L_y^2} + \frac{1}{L_z^2}\right)$
Coats (1989)	$8\left(\frac{1}{L_x^2}\right)$	$8\left(\frac{1}{L_x^2} + \frac{1}{L_y^2}\right)$	$8\left(\frac{1}{L_x^2} + \frac{1}{L_y^2} + \frac{1}{L_z^2}\right)$
Chang (1993) constant pressure; Lim & Aziz (1995)	$\pi^2\left(\frac{1}{L_x^2}\right)$	$\pi^2\left(\frac{1}{L_x^2} + \frac{1}{L_y^2}\right)$	$\pi^2\left(\frac{1}{L_x^2} + \frac{1}{L_y^2} + \frac{1}{L_z^2}\right)$
Chang (1993) constant flow rate	$12\left(\frac{1}{L_x^2}\right)$	$12\left(\frac{1}{L_x^2} + \frac{1}{L_y^2}\right)$	$12\left(\frac{1}{L_x^2} + \frac{1}{L_y^2} + \frac{1}{L_z^2}\right)$
Quintard & Whitaker (1995)	$12\left(\frac{1}{L_x^2}\right)$	$14.22\left(\frac{1}{L_x^2} + \frac{1}{L_y^2}\right)$	$16.54\left(\frac{1}{L_x^2} + \frac{1}{L_y^2} + \frac{1}{L_z^2}\right)$
Sarda et al. (2002)	$\frac{8}{L^2}$	$\frac{24}{L^2}$	$\frac{48}{L^2}$
Different geometries			
Lim & Aziz (1995)	-	$\sigma_{cylinder} = \frac{5.78}{r^2}$	$\sigma_{sphere} = \frac{\pi^2}{r^2}$
Kazemi & Gilman (1992)	-	-	$\sigma_{cylinder} = \frac{4}{h^2} + \frac{2}{r^2}$

Table 1: Overview of Shape Factors in the Literature

\* for  $n=2$ ,  $l = \frac{3L_x L_y L_z}{L_x L_y + L_x L_z + L_y L_z}$ ;  $n=3$ ,  $l = \frac{2L_x L_y}{L_x + L_y}$

## CHAPTER 3

### METHODOLOGY

#### 3.1 Overview of Research Methodology

Research works and the corresponding methodologies were summarized in the table below.

Research Works	Methodologies
Preliminary Research & Background Study	a) Literature Review
Analyze the computation modules in a dual porosity naturally fractured reservoirs (NFR) simulator	a) Programming codes in NFR simulator was analyzed and the program sequence flow chart (Figure 5 - Figure 7) was produced. b) Minor debugging has been done on the NFR computation via pressure explicit method.
Selects an appropriate base case model and parameters for comparison study.	a) Various base cases were studied and 2 base cases were selected for the comparison studies. Details on the selected base cases can be found at Section 3.5 b) Appropriate fractures length for comparison study was selected. Fractures length selection was explained in Section 3.7.
Study the derivation of different	a) Various geometry of shape factors were

leakage terms for matrix and fracture	<p>derived using Kazemi's Generalized Shape Factor Equations.</p> <p>b) Various types of transfer functions found in the literature were studied.</p> <p>c) Rangel-German &amp; Kavscek (2005) transfer function was further elaborated to ease the implementation onto NFR simulator.</p>
Implements different leakage coefficients into NFR simulator and compares the results	<p>a) Various shape factors were implemented into the NFR simulator.</p> <p>b) Rangel-German &amp; Kavscek (2005) transfer function and Sarma &amp; Aziz (2006) transfer function were implemented into the NFR simulator.</p>
Generate appropriate NFR simulator output for visualization	<p>a) NFR simulator was modified to generate required data set for visualization.</p> <p>b) Generated data set can be processed by visualization software to produce animation of the results.</p>

Table 2: Summary of Research Works and Methodologies

### 3.2 Research Flow Chart

This research can be divided into 5 phases corresponding to the scope of work and methodologies. The 5 phases are:

Phase 1: Background study and literature review.

Phase 2: Selection and analysis of NFR simulator software.



Phase 3: Comparison approach.

Phase 4: Post processing and visualization.

Phase 5: Discussions and conclusions.

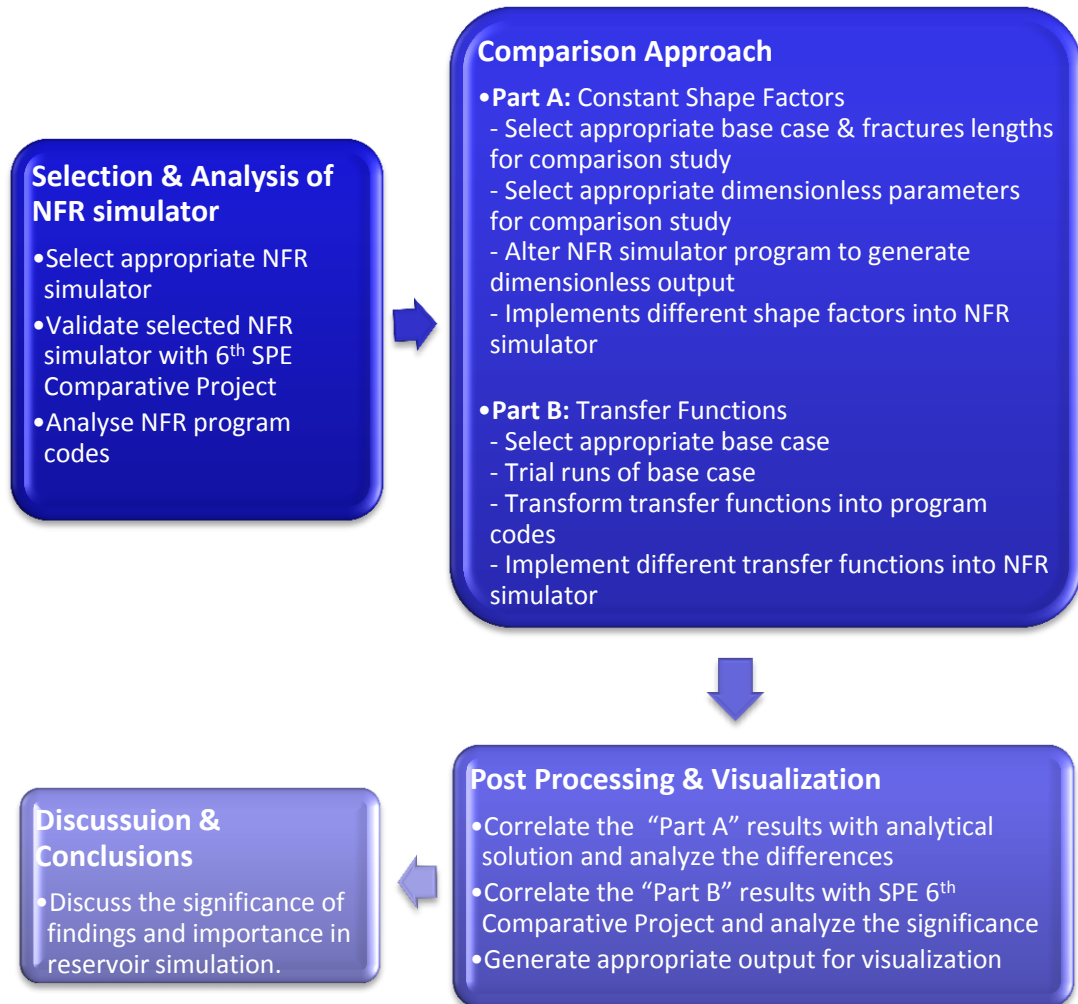


Figure 4: Research Flow Chart

### 3.3 Program flow chart of NFR simulator

The program flow chart of the NFR simulator software (Figure 5 - Figure 7) consists of 22 main modules. The first 4 modules which are Input Data, Transmissibility, Faults, and Initialization were only run once in the NFR simulator software. The remaining 18 modules were run in a loop for calculations until the simulation run time reached the time limit set by user. Details on each module functions were briefly described in the flow chart.

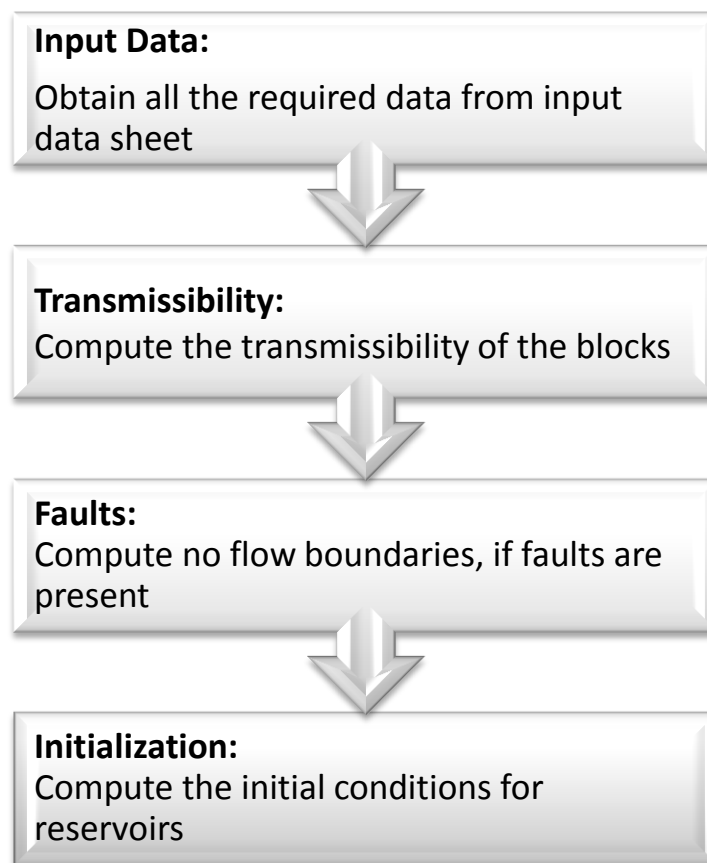


Figure 5: NFR Simulator Program Flow Chart, module 1 to 4.

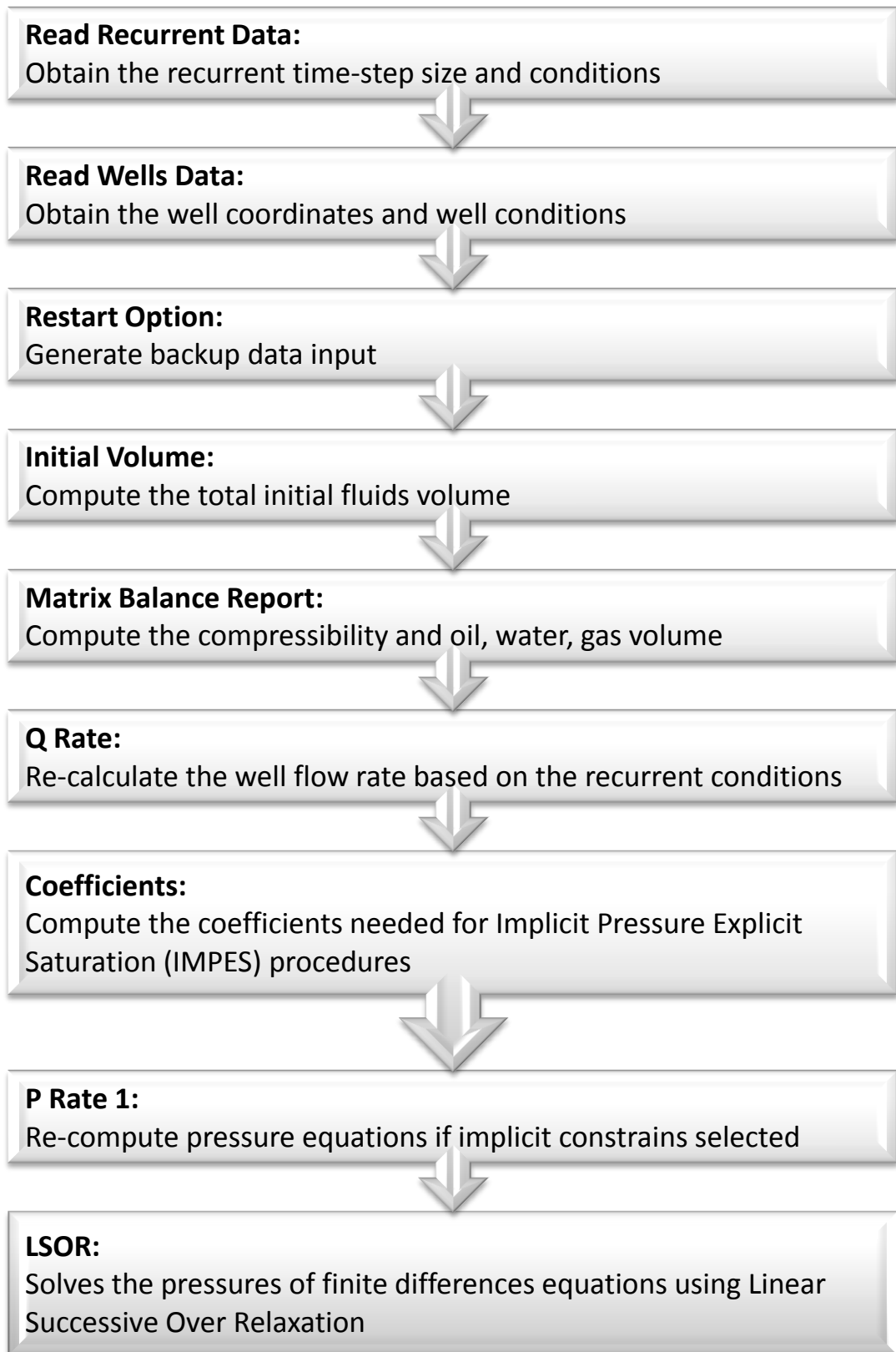


Figure 6: NFR Simulator Program Flow Chart, module 5 to 13.

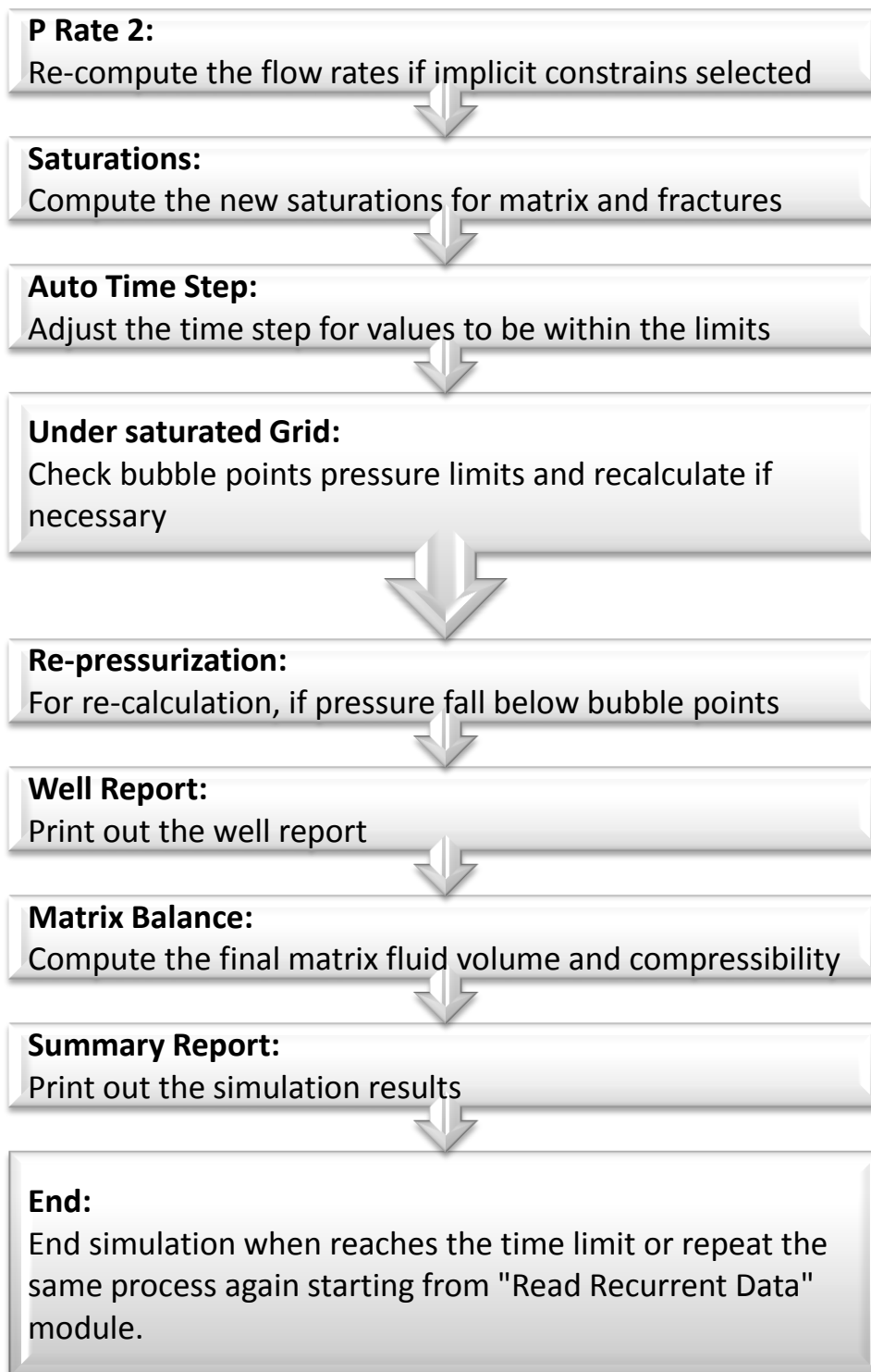


Figure 7: NFR Simulator Program Flow Chart, module 14 to 22.

### 3.4 Brief Descriptions of the Selected NFR Simulator Software

The selected NFR simulator uses dual porosity concepts, whereby matrix and fractures are computed separately, which later linked together by a transfer function. The NFR simulator uses effective permeability and porosity concepts in each block. This means that the fractures properties and matrix properties are same within the block but not necessary the same in another block. Thus, users can simulate heterogenous reservoir problems by separating matrix-fractures of different properties into another blocks.

Matrix block with 3 set of fractures means that there are interconnected fractures in every directions. Therefore, water, oil, or gas can transfer through matrix in X, Y, and Z directions (Figure 8). Matrix block with 2 set of fractures means that there are interconnected fractures in only 2 directions which could be X-Y, Y-Z, or X-Z directions (Figure 9). As well as the matrix with single set of fractures, there are interconnected fractures in only 1 direction which could be X,Y, or Z direction (Figure 10).

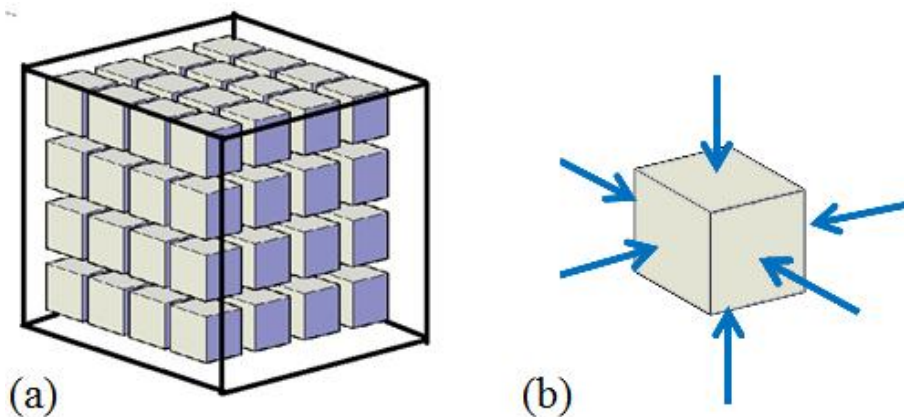


Figure 8: (a) A matrix block with 3 set of fractures (b) crosssection of matrix showing the flow mechanism

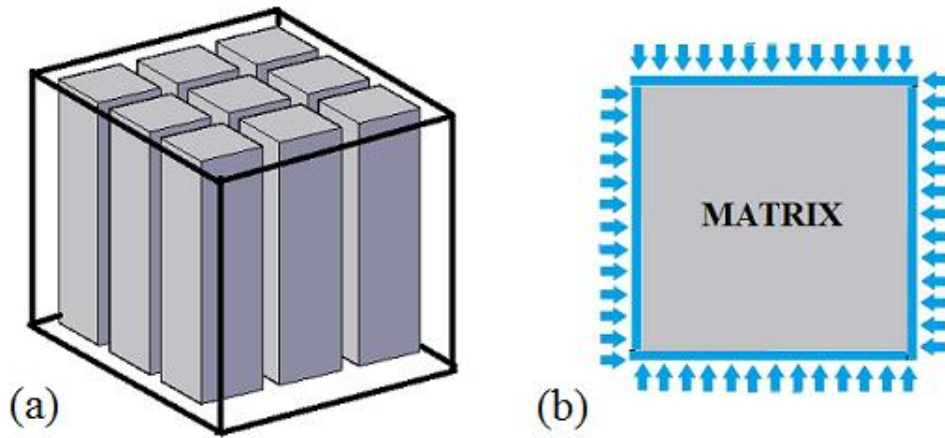


Figure 9: (a) A matrix block with 2 set of fractures (b) crossection of matrix showing the flow mechanism

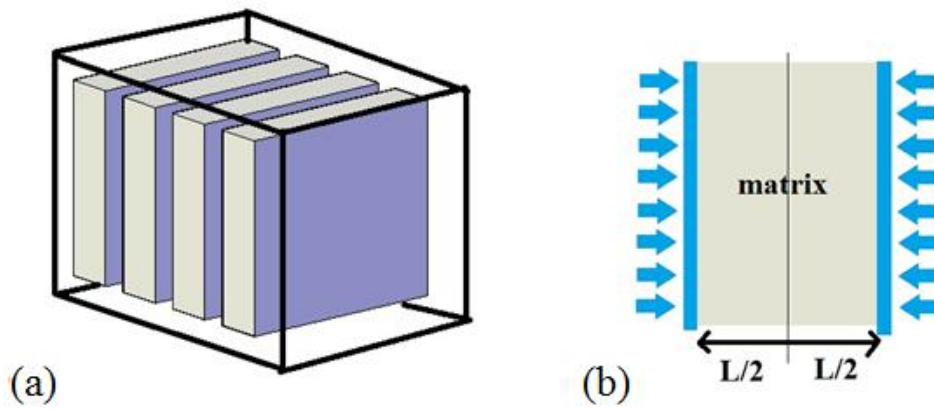


Figure 10: (a) A matrix block with 1 set of fractures (b) crossection of matrix showing the flow mechanism

### 3.5 Gantt Chart and Milestone

#### 3.5.1 Final Year Project 1

	WEEK NO.	1	2	3	4	5	6	7	8	9	10	11	12	13	14
1	<b>Title Registration</b>														
2	<b>Literature Review</b>														
3	<b>Extended Proposal</b>														
4	<b>Proposal Defense</b>														
5	<b>Interim Report</b>														
6	<b>Weekly Progress Presentation</b>														
7	<b>Selection of Base Case Model</b>														
	a. Familiarization with NFR software														
	b. Comparison of different base case models														
	c. Selection of an appropriate base case model														
8	<b>Derivation and Implementation of different leakage coefficients into NFR software</b>														

Milestone  


Table 3: Final Year Project 1 Gantt chart

### 3.5.2 Final Year Project 2

WEEK NO.	1	2	3	4	5	6	7	8	9	10	11	12	13	14
<b>8</b>	<b>Derivation and Implementation of different leakage coefficients into NFR software</b>													
<b>9</b>	<b>Sensitivity Analysis of Result</b>													
	a. Examine the significance of the result													
	b. Validating the result													
<b>10</b>	<b>Progress Report</b>													
<b>11</b>	<b>Draft Report</b>													
<b>12</b>	<b>Discussion of Result</b>													
<b>13</b>	<b>Generate Result Visualization</b>													
<b>14</b>	<b>Project Dissertation (Soft bound)</b>													
<b>15</b>	<b>Technical Paper</b>													
<b>16</b>	<b>Project Dissertation (Hard bound)</b>													

Milestone



Table 4: Final Year Project 2 Gantt chart



### 3.6 Selection of Base Cases

#### 3.6.1 Comparison of constant shape factor

Several problems were run and the problem selected for this study was a depletion run with 5x3x2 blocks and only one production well at (1, 1, 1). 5x3x2 blocks were selected for this purpose to allow 3 dimensional flows between matrix blocks during simulation. One production well was selected to avoid complication of the problems which later would complicate the results analysis. The production runs with no flow constraints, 5500 psi bottom hole pressure, and PID index of 1. Table 5 describes the details of the base case. The reservoir fluid data is on Table 9- Table 14. Meanwhile, selection for the appropriate size of fractures length is discussed in Section 3.7.

Number of blocks, $n_x, n_y, n_z$	$5 \times 3 \times 2$
Blocks dimension, $ft$	$100 \times 100 \times 100$
Matrix porosity, $fraction$	0.29
Matrix permeability, $md$	1
Fracture porosity, $fraction$	0.01
Fracture permeability, $md$	90

Table 5: Basic data for depletion run.

#### 3.6.2 Comparison of transfer function

Comparisons of transfer functions require water injection cases. Therefore, it is best to use the base case from the SPE 6<sup>th</sup> Comparative Solution Project (1990). The base case of blocks with water-injection was selected for the comparison study. The case descriptions are on Table 6 – Table 8.

Number of blocks, $n_x, n_y, n_z$	$10 \times 1 \times 5$
Blocks dimension, $ft$	$200 \times 1000 \times 50$
Matrix porosity, $fraction$	0.29

Matrix permeability, <i>md</i>	1
Matrix Z-direction permeability, <i>md</i>	0.1
Fracture porosity, <i>fraction</i>	0.01

Table 6: Basic data for water-injection case\*

Layer	Fracture permeability, <i>md</i>	Fracture Z-direction permeability, <i>md</i>	Productivity Index, J <i>RB · cp / Days · psi</i>
1	10	1	1
2	10	1	1
3	90	9	9
4	20	2	2
5	20	2	2

Table 7: Layer data\*

Wells	XY Coordinates	Perforation	Total Fluid (Oil + Water) Production Rate	Injection Rate
Oil production	(1,1)	Layer 1,2,3	1000 STB/D	-
Water-injection	(10,1)	Layer 1,2,3,4,5	-	1750 STB/D

Table 8: Wells information\*

\*Data were obtained from Firoozabadi & Thomas (1990), SPE 6<sup>th</sup> Comparative Solution Project.

### 3.6.3 Reservoir Properties

Both of the comparison studies use same reservoir properties. The reservoir properties are described in Table 9- Table 14.

Initial reservoir pressure, <i>psi</i>	6000
Initial oil saturation in matrix, <i>fraction</i>	0.8
Initial water saturation in matrix, <i>fraction</i>	0.2

Initial oil saturation in fracture, <i>fraction</i>	1
Initial water saturation in fracture, <i>fraction</i>	0
Connate water saturation, <i>fraction</i>	0.2
Residue oil saturation, <i>fraction</i>	0.25
Rock compressibility, <i>psi</i> <sup>-1</sup>	$3.5 \times 10^{-6}$
Oil bubble point pressure, <i>psi</i>	5545
Slope of oil viscosity above bubble point, $\partial\mu/\partial u$ , <i>cp/psi</i>	$1.72 \times 10^{-5}$
Oil formation volume factor at bubble point	1.8540
Slope of formation volume factor above bubble point, $\partial B_o/\partial p$ , <i>RB/STB/psi</i>	$-4.0 \times 10^{-5}$

Table 9: Basic Reservoir Properties\*\*

Oil Density, <i>lb/ft</i> <sup>3</sup>	Water Density, <i>lb/ft</i> <sup>3</sup>	Gas Density, <i>lb/ft</i> <sup>3</sup>
51.14	65	0.058

Table 10: Density of oil, water, and gas at standard condition\*\*

Phase saturation	Oil relative permeability, KRO	Water relative permeability, KRW	Gas relative permeability, KRG	Pressure capillary oil/water, PCOW	Pressure capillary gas/oil, PCGO
0	0	0	0	1	0
0.1	0	0	0.015	1	0
0.2	0	0	0.05	1	0
0.25	0	0.005	0.0765	0.5	0
0.3	0.042	0.01	0.103	0.3	0
0.35	0.1	0.02	0.1465	0.15	0
0.4	0.154	0.03	0.19	0	0
0.45	0.22	0.045	0.25	-0.2	0
0.5	0.304	0.06	0.31	-1.2	0
0.6	0.492	0.11	0.538	-4	0
0.7	0.723	0.18	0.538	-10	0
0.75	0.86	0.23	0.538	-40	0
0.8	1	0.23	0.538	-40	0
1	1	0.23	0.538	-40	0

Table 11: Relative permeability data\*\*

Pressure, psia	Oil Viscosity, cp	Oil formation volume factor, RB/STB	Solution gas-oil ratio, SCF/STB RSO
1674	0.529	1.3001	367
2031	0.487	1.3359	447
2530	0.436	1.3891	564
2991	0.397	1.4425	679
3553	0.351	1.5141	832
4110	0.31	1.5938	1000
4544	0.278	1.663	1143
4935	0.248	1.7315	1285
5255	0.229	1.7953	1413
5545	0.21	1.854	1530
7000	0.109	2.1978	2259

Table 12: Saturated oil properties\*\*

Pressure, psia	Water viscosity, cp	Water formation volume factor, RB/STB	Solution gas-water ratio, SCF/STB
1674	0.35	1.07	0
7000	0.35	1.09	0

Table 13: Water properties\*\*

Pressure, psia	Gas viscosity, cp	Gas formation volume factor RCF/SCF
1674	0.0162	0.0111177
2031	0.0171	0.0090963
2530	0.0184	0.0072995
2991	0.0197	0.00623265
3553	0.0213	0.005384785
4110	0.023	0.004800825
4544	0.0244	0.004463925
4935	0.0255	0.004216865
5255	0.0265	0.0040428
5545	0.0274	0.00390804
7000	0.033	0.003369

Table 14: Gas properties\*\*

\*\*All the properties used in simulation were taken from Almengor et al. (2002), BOAST-NFR manual which are the same with Firoozabadi & Thomas (1990), SPE 6<sup>th</sup> Comparative Solution Project.

### 3.7 Derivation of Kazemi Shape Factor for Various Geometries.

Shape factor is closely related with geometries. Therefore, it is useful to compare different geometries of shape factors. Lim & Aziz (1995) has provided cylindrical, rectangular, and sphere geometries shape factors. It is best to have another researcher's shape factor to do comparisons and analyze the effect of different geometries. For this purposes, Kazemi's generalized shape factor equation is used to various geometries shape factors. The Kazemi's generalized shape factor was given in the Eq. (2.8). Summary of different geometries shape factors is given in Table 15. Equivalent fractures length of each geometries can be found by using same volume constrains.

#### 3.7.1 Kazemi's cylinder shape factor

It is given in the literature that cylinder with all side of imbibition shape factor is

$$\begin{aligned}\sigma_s &= \frac{1}{\pi r^2 h} \left[ \frac{2\pi r h}{r} + \frac{\pi r^2}{0.5h} + \frac{\pi r^2}{0.5h} \right] \\ \sigma_s &= \frac{4}{h^2} + \frac{2}{r^2}\end{aligned}\quad (3.1)$$

This cylinder shape factor can be re-written in the form of :

$$\sigma_s = 4 \left[ \frac{1}{h^2} + \frac{1}{2r^2} \right] \quad (3.2)$$

When the height of cylinder approaches to infinite, the shape factor can further reduced into 2D problems. Whereby,

$$\begin{aligned}h &\rightarrow \infty; \\ \sigma_s &= 2 \left[ \frac{1}{r^2} \right]\end{aligned}\quad (3.3)$$

#### 3.7.2 Kazemi's sphere shape factor

For sphere, the shape factor is

$$\sigma_s = \frac{3}{4\pi r^3} \left[ \frac{4\pi r^2}{r} \right]$$

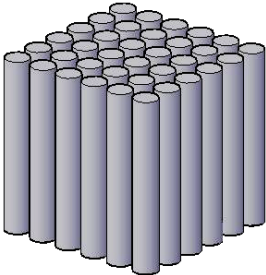
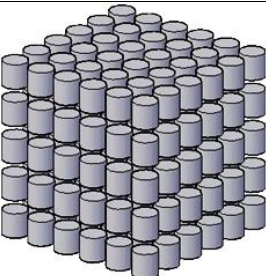
$$\sigma_s = 3 \left[ \frac{1}{r^2} \right]$$
(3.4)

### 3.7.3 Kazemi's tetrahedron shape factor

Volume of tetrahedron =  $\frac{\sqrt{2}}{12} a^3$ ; Surface area of each sides =  $\frac{\sqrt{3}}{4} a^2$ ; Height =  $\frac{\sqrt{2}}{\sqrt{3}} a$

$$\sigma_s = \frac{12}{\sqrt{2}a^3} \left[ \left( \frac{\sqrt{3}a^2}{4} \right) \left( \frac{2\sqrt{3}}{\sqrt{2}a} \right) (4) \right]$$

$$\sigma_s = 36 \left[ \frac{1}{a^2} \right]$$
(3.5)

Geometries	Kazemi & Gilman (1992)	Lim & Aziz (1995)
 Circle (2 set fractures)	$2 \left( \frac{1}{r^2} \right)$	$\frac{5.78}{r^2}$
 Cylindrical (3 set fractures)	$4 \left( \frac{1}{h^2} + \frac{1}{2r^2} \right)$	N/A

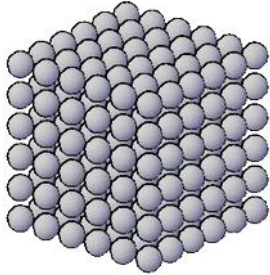
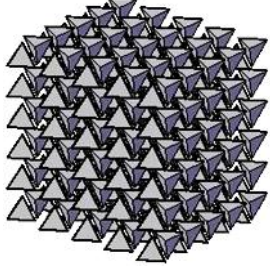
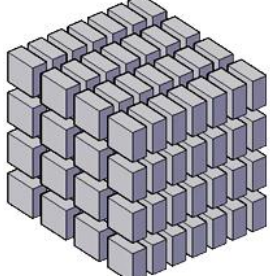
 <p>Sphere (3 set fractures)</p>	$3\left(\frac{1}{r^2}\right)$	$\frac{\pi^2}{r^2}$
 <p>Tetrahedron (3 set fractures)</p>	$36\left(\frac{1}{a^2}\right)$	<p>N/A</p>
 <p>Rectangular (3set fractures)</p>	$4\left(\frac{1}{L_x^2} + \frac{1}{L_y^2} + \frac{1}{L_z^2}\right)$	$\pi^2\left(\frac{1}{L_x^2} + \frac{1}{L_y^2} + \frac{1}{L_z^2}\right)$

Table 15: Summary of different geometries shape factors.

## **CHAPTER 4**

### **VALIDATIONS OF NFR SIMULATOR SOFTWARE**

Validation of NFR simulator software is to verify the reliability of simulated results. Validation helps to determine if the NFR simulator software is suitable to be used for this comparison study. For the verification purpose, the NFR simulator results are to be compared with water-injection case of SPE 6<sup>th</sup> Comparative Solution Project: Dual Porosity Simulators, 1990.

#### **4.1 Verifications of the Selected NFR Simulator**

A quick comparison is done by superimpose the NFR simulator results with the results of several companies that have participated in the SPE 6<sup>th</sup> Comparative Solution Project: Dual Porosity Simulators, 1990. The Figure 11 shows the comparison of results. The dotted lines represent the NFR simulator results. This showed that the simulator result using the original Warren & Root (1963) transfer function was very much conservative. There are many possible factors that contributed to this deviation of results. One of the identified factors is there is no additional imbibition term taken into account. However, an imbibition term is important only when involving injections cases and it can be negligible for depletion cases. Therefore, no modifications needed to be done for depletion case study. Meanwhile, there are many possibly rooms of improvement for this NFR simulator by implementing modern transfer functions. For the purpose, two transfer functions (Rangel-German & Kovsky, 2005; Sarma & Aziz, 2006) have been identified for implementation into this NFR simulator. Section 5.3.1 will demonstrate the improvements on NFR simulator after implementing the modern transfer functions.



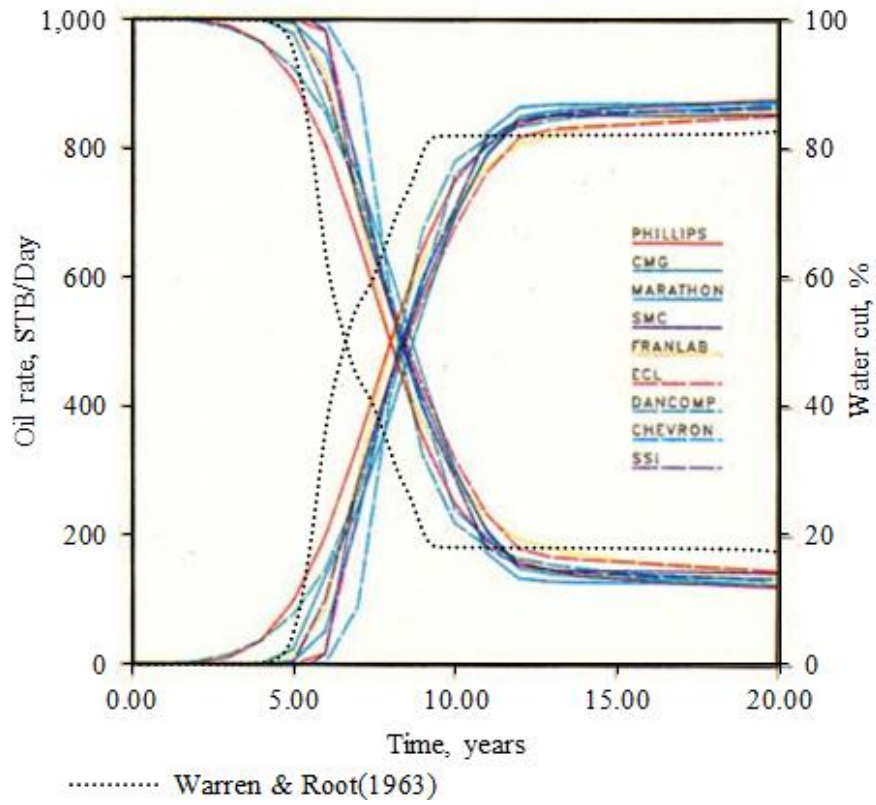


Figure 11: Simulation result of basic double porosity NFR simulator. The transfer function in the simulator is from Warren & Root (1963).

## CHAPTER 5

### RESULTS & DISCUSSION

#### 5.1 Comparison of Shape Factor

Lim & Aziz (1995) has provided analytical derivation of shape factors for single phase flow. In the effort of deriving shape factors, they have showed that the total amount of mass entered a system at time  $t$ ,  $M_t$  and the corresponding mass after an infinite time,  $M_\infty$  can be expressed as in Eq. (2.16). The Eq. (2.16) is known as a dimensionless pressure,  $P_d$ . This dimensionless pressure is a function of dimensionless time Eq. (5.1), and the analytical expressions for single phase flow are shown in the Eq. (2.17-2.20).

$$t_d = \frac{kt}{\phi\mu c_i L^2} ; \text{gradient} = \frac{\delta P_d}{\delta t_d} \quad (5.1)$$

It is desired to know the effect of different shape factors in multiphase flow NFR simulation. The comparison is done by representing the simulation results in  $P_d$  and  $t_d$ . A basic double porosity simulator is used to solve the reservoir problem. The simulator solves the pressure and saturation by using Implicit Pressures Explicit Saturation (IMPES) method. When  $P_d$  is plotted against  $t_d$ , the gradient ( $P_d/t_d$ ) gives indication of the matrix-fracture transfer rate. From Eq. (5.2), it is shown that the matrix-fracture transfer rate is proportional to the gradient ( $P_d/t_d$ ). Eq. (5.2) can be found by extending the analytical solution given by Lim & Aziz (1995). The derivation new correlation is shown in the appendix.

$$\tau_{mf} = \frac{\partial p_d}{\partial t_d} \left( \frac{\rho k}{\mu L^2} (p_i - p_f) \right) \quad (5.2)$$

This relation is very useful for analyzing the results. In additions, the results are compared against the analytical solutions from Lim & Aziz (1995).

### 5.1.1 Single Set of Fractures

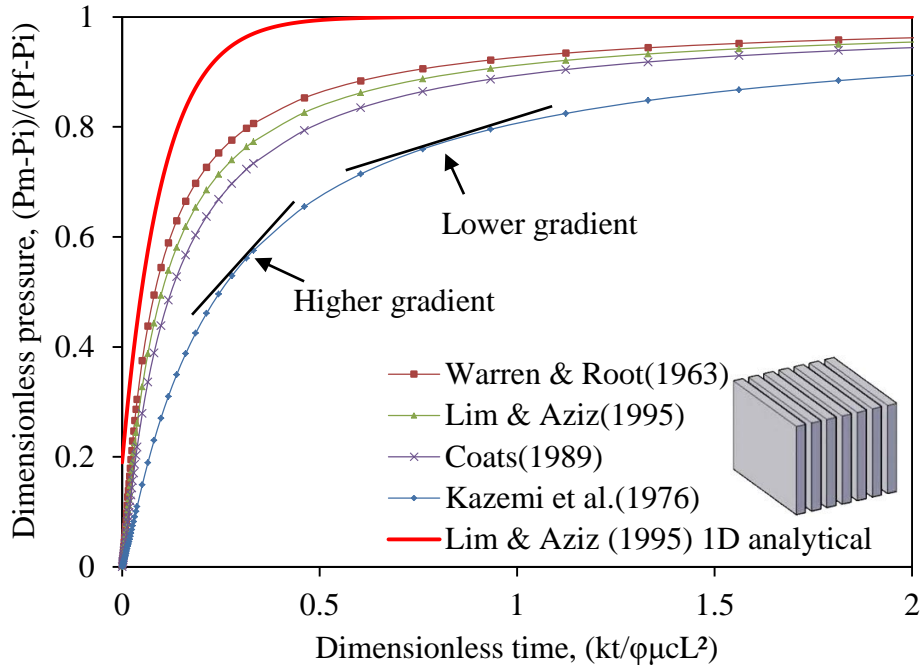


Figure 12: Single set of fractures: Dimensionless pressure vs dimensionless time

The comparison result for single set of fractures is presented in Figure 12. By applying Eq. (5.2), it is deduced that steeper gradient shows higher matrix-fracture transfer rate. At  $t_d < 0.5$ , Kazemi's shape factor has showed much lower transfer rate as compared with other researcher's shape factor. It also require twice the  $t_d$  value to reach the same  $P_d$  value. Note that the curve gradient is very high at early  $t_d$  and becoming lower as  $t_d$  increases (Figure 12). Eq. (5.3) is the rate of change of gradient.

$$\Delta \text{ gradient} = \frac{\partial^2 P_d}{\partial t_d^2} \quad (5.3)$$

Conversely, Warren & Root(1963) shape factor yield the highest  $\Delta \text{gradient}$ . The Warren & Root(1963) shape factor transfer rate is the highest at early  $t_d$ , and then, the transfer rate dropped quickly. In general, all the results converges into  $P_d \approx 1$ . As curve  $\Delta \text{gradient} \rightarrow 0$ , it means that the matrix-fracture transfer rate is becoming steady. When the gradient is 0, it literally means that no flow between matrix-fracture and it occurs at  $P_d=1$ . At  $P_d=1$ , the  $p_m$  must be equal to  $p_f$  since the initial

pressure,  $p_i$  always constant. This is in agreement with the Eq. (1.1), whereby there must be a pressure difference to initiate flow.

As stated earlier, analytical solution from Lim & Aziz (1995) is based on single phase flow and direct comparison cannot be made. However, it can be observed that the analytical solutions has much higher  $\Delta gradient$  as compared with others. This denotes that the analytical solutions transfer rate is very high at initial  $t_d$  and then decreases rapidly. The reservoir problem is a multiphase flow problem whereby the transfer of fluids are much more complex. The components that present in a multiphase flow is water, oil, and gas. Plus, the total multiphase matrix-fracture transfer rate is a summation of all the components. Meanwhile, single phase matrix-fracture transfer rate is having only the oil components. Analytical solution cannot be compared directly with results of other shape factors but it can serves as a reference line. This can be used to detect shape factor results that yield faster transfer rate by comparing the gradient and  $P_d$ .

### 5.1.2 Double set of fractures & Triple set of fractures

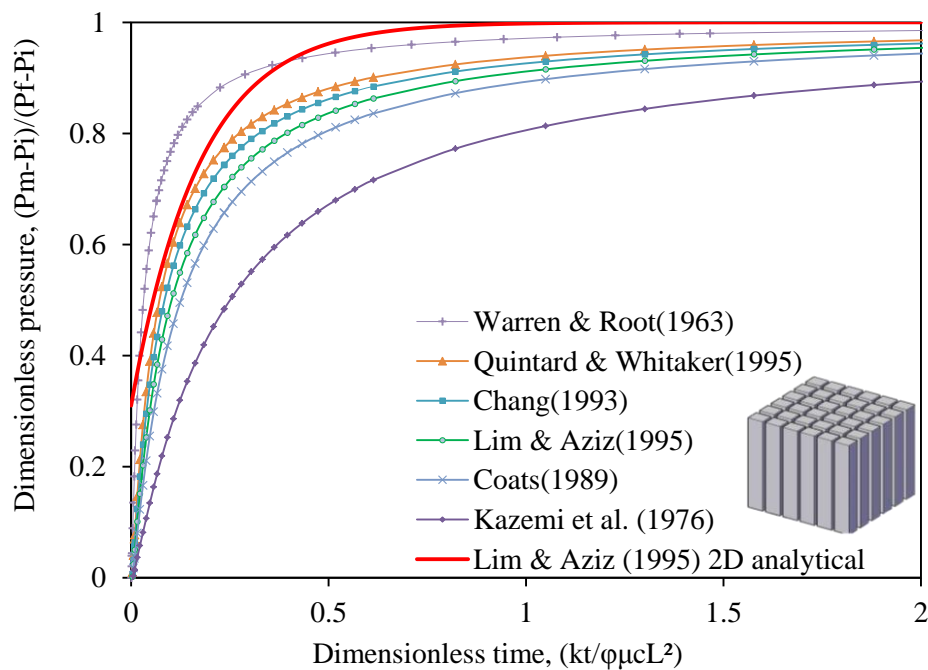


Figure 13: Double set of fractures: Dimensionless pressure vs dimensionless time

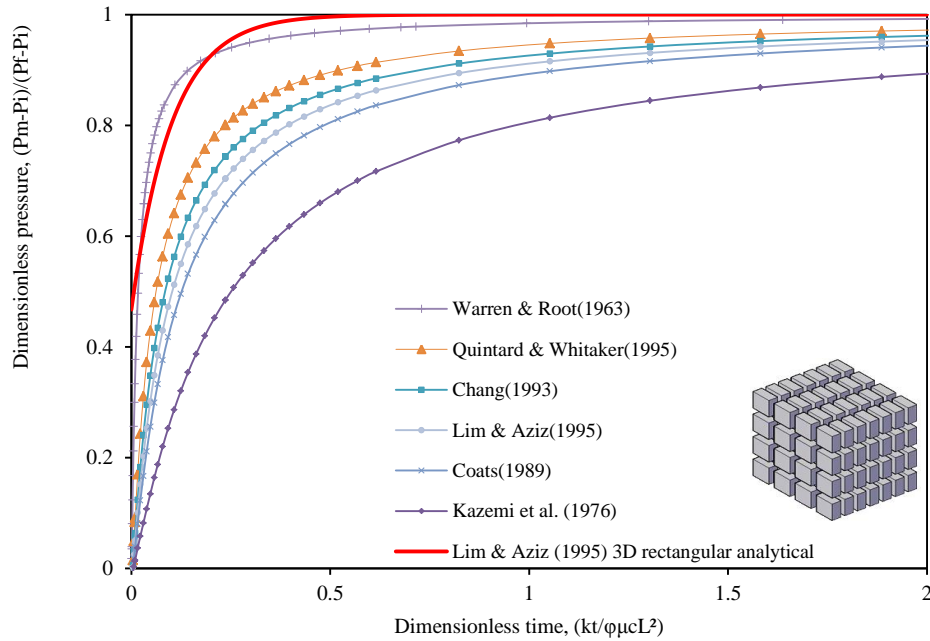


Figure 14: Triple set of fractures: Dimensionless pressure vs dimensionless time

The comparison result for double set of fractures is presented in Figure 13 and comparison result for triple set of fractures is presented in Figure 14. Both of the results can be analyzed by using the same approach discussed in Section 5.1 and Section 5.1.1. It is interesting to note that at initial  $t_d$ , Warren & Root (1963) shape factor yield higher transfer rate as compared with the analytical solution. This indicate that Warren & Root (1963) shape factor has higher matrix-fracture transfer rate prediction as compared to Lim & Aziz (1995) single phase analytical solution and other shape factors. In general, Warren & Root (1963) has the highest  $\Delta gradient$ , then followed by Lim Quintard & Whitaker (1995), Chang (1993) constant volume shape factor, Lim & Aziz (1995), Coats (1989), and Kazemi (1976).

### 5.1.3 Different geometries

Different geometries shape factors are available for 2 set of fractures and 3 set of fractures (Table 15). The circle geometry shape factor is based on 2 set of fractures, while sphere, cylindrical, rectangle, and tetrahedron is based on 3 set of fractures. The results can be analyzed by using the same approach discussed in Section 5.1.1.

The singlephase analytical solutions for 2 set and 3 set of fractures are plotted in the Figure 15 as for comparison purpose.

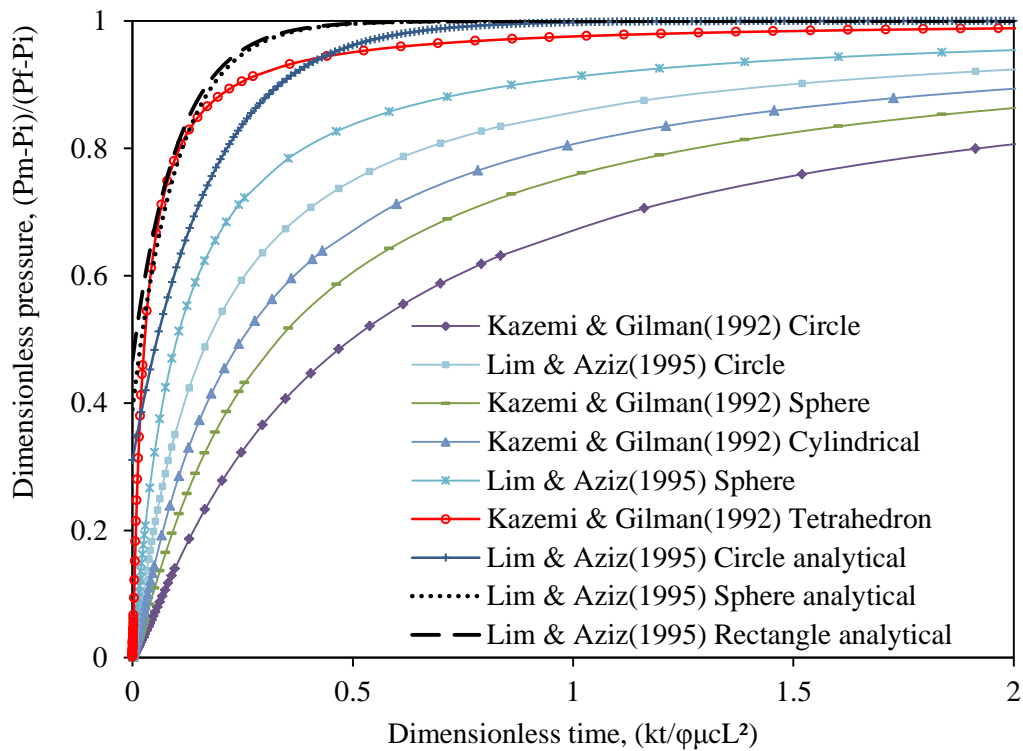


Figure 15: Various geometries: Dimensionless pressure vs dimensionless time

Summary, Kazemi & Gilman(1992) circle shape factor has the lowest  $\Delta gradient$ , followed by Kazemi & Gilman(1992) sphere, Kazemi & Gilman(1992) cylindrical, Lim & Aziz (1995) circle, Lim & Aziz (1995) sphere, and Kazemi & Gilman (1992) tetrahedron.

## 5.2 Importance of the comparison

Previously it is discussed and showed in Section 5.1.1, Warren & Root (1963) has the highest transfer rate at initial  $t_d$  and then transfer rate will drop quickly as compared with other shape factors. By knowing higher value of shape factor will results in initial high transfer rate between matrix-fracture and then followed by quick drop of transfer rate, the simulation trend with different shape factors can be predicted. This is can be useful for history matching. Figure 16 is example of separate simulation results with different shape factors and it follows the trend. Note

that the simulation case problem is 15x1x1 blocks with water injection and oil production. It is different from one used in the comparison study.

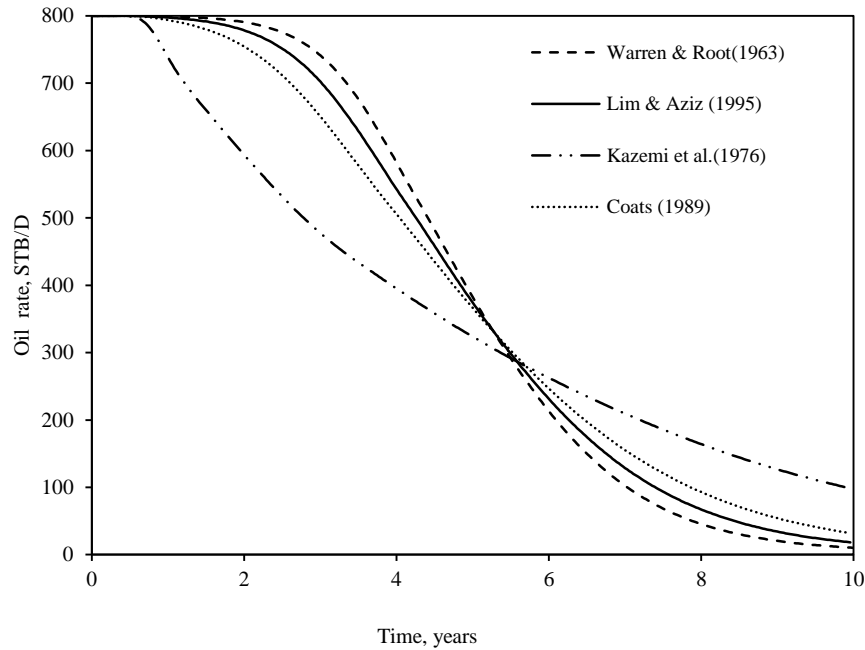


Figure 16: Simulation of 15x1x1 blocks with water injection & oil production with different researcher's shape factor (single set of fractures). The problem is taken from BOAST-NFR manual. BOAST-NFR uses Lim & Aziz (1995) shape factor.

### 5.3 Comparison of time dependent transfer functions

Rangel-German & Kovscek (2005) and Sarma & Aziz (2005) has provided time dependent transfer functions that properly accounts for water imbibition. Both of the time dependent transfer functions can be implement into double porosity/double permeability models without requiring major modifications. The implementations are straight forward but it still requires a proper understanding of corresponding simulator programs. For double porosity simulator that uses IMPES method, the recalculation of pressure and saturation should account for the new water transfer rate between matrix-fracture. This usually can be done by examining the pressure module and saturation module of simulator. However, the implementations can vary and it depends on the type of simulator.

### 5.3.1 Verifications & comparison of results

The initial simulation using the Warren & Root (1963) transfer function lead to pessimistic recovery prediction (Figure 11). This is in agreement with both of the researchers' claims (Rangel-German, 2002, Sarma & Aziz, 2006). It is observed that the maximum oil flow rate of 1000 STB/D only lasted for about 5 years before the production well start producing water. This possibly indicates that the transfer function does not sufficiently accounts for water imbibition into matrix rock.

Additional simulations are repeated by using different transfer functions. Rangel-German & Kovscek (2005) and Sarma & Aziz (2006) transfer functions are implemented into the basic double porosity NFR simulator. Besides, we also consider the combination of the two transfer functions (Eq. 5.4) and it is also implemented into the simulator.

$$q_w = \sigma_p V \frac{\bar{K}k_{rw}}{\mu_w} (\bar{p}_{wm} - p_{wf}) - Q_{w_{avg}} \quad (5.4)$$

$$Q_{w_{avg}} = \left[ \frac{\sigma_s VD_h (S_{w_{max}} - \bar{S}_{wm}) + V\phi\sigma_{SD} (\bar{S}_w - S_{wi})}{2} \right] \quad (5.5)$$

*In all the simulations, shape factor  $\sigma_p$  used is  $\pi^2 / L^2$  (Lim & Aziz, 1995).*

Figure 17 shows the simulation results by using 3 different transfer functions. It is observed that double porosity simulation using the time dependent transfer function (Eq. 26, Eq. 29, and Eq. 32) has a better matching with the water injection result from Sixth SPE Comparative Solution Project (Firoozabadi & Thomas, 1990). The maximum oil flow rate of 1000 STB/D lasted for about 6 years before the production well start producing water. It has a much better recovery estimate. The Rangel-German & Kovscek (2006) transfer function has the highest recovery estimate, followed by the combination of two (Eq. 32), and then Sarma & Aziz (2006). These transfer functions have better accounts for matrix-fracture transfer rate involving wetting phase (water) imbibition.



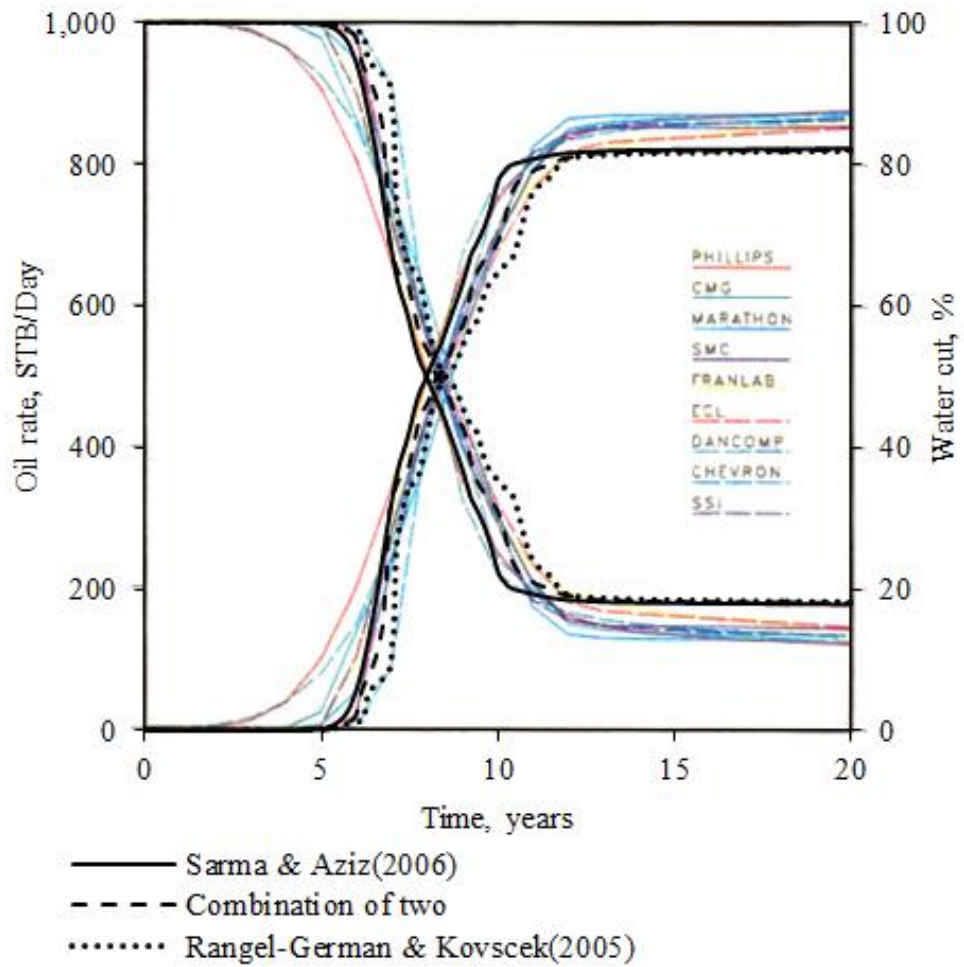


Figure 17: Simulation result of double porosity NFR simulator with 3 different transfer functions.

Visualization of the water saturation profile in reservoir blocks for the simulation is available in the appendix section.

## CHAPTER 6

### CONCLUSION & RECOMMENDATION

#### 6.1 Conclusion

i. Comparison of shape factors in multiphase problem is presented in dimensionless parameters,  $P_d$  and  $t_d$ . Gradient  $P_d / t_d$  is proportional to the matrix-fracture transfer rate. Therefore, higher gradient  $P_d / t_d$  indicate higher transfer rate. The dimensionless comparison displays the different flow behavior of different shape factors. This provides better understanding regarding the differences among different shape factors.

ii. Different transfer functions are compared by using water injection problem from Sixth SPE Comparative Solution Project (Firoozabadi & Thomas, 1990). The comparison showed direct generalization of the classical transfer function is insufficient especially when injection case present. Instead, the time dependent imbibition term in transfer function should be considered in modeling NFR. Failure to consider would lead to erroneous and pessimistic recovery.

#### 6.2 Recommendations

i. A new correlation (Eq. 5.2) is derived to relate the dimensionless terms. This correlation is does not require shape factor and it is similar with Sarma & Aziz (2006) time dependent shape factor Eq. (2.34). Direct implementation of the new correlation into general double porosity model is not feasible as it requires defining the dimensionless terms. Suggested future work could be creating a new model that uses this correlation as a transfer function.

ii. Another future comparison of shape factor can be done using the same parameters except the oil residue, water connate saturation, and water maximum saturation in rock matrix. The purpose is to investigate on how the initial saturation and shape factor will influence the matrix-fracture transfer rate.

## NOMENCLATURE

### Nomenclature

$t$	time, T
$L$	length, L
$V$	volume, $L^3$
$A$	area, $L^2$
$q$	transfer rate, $L^3/T$
$Q$	transfer rate, M/T
$\tau$	transfer rate, M/ ( $L^3T$ )
$p$	pressure, M/( $LT^2$ )
$k$	permeability, $L^2$
$\sigma$	shape factor, $1/L^2$
$\mu$	viscosity, M/(LT)
$n$	Corey function
$D$	diffusivity, $L^2/T$
$\phi$	porosity, fraction
$s$	saturation, fraction
$c$	compressibility, fraction
$x$	x-direction
$y$	y-direction
$z$	z-direction
$h$	height, L
$r$	radius, L
$a$	side of tetrahedron, L
$\lambda$	fluid mobility, ( $L^3T$ )/M
$\rho$	density, M/ $L^3$

### Subscripts

$i$	initial
$w$	water
$o$	oil
$g$	gas
$m$	matrix
$f$	fracture
$t$	total
$h$	hydraulic
$c$	corrected
$\infty$	infinity
$d$	dimensionless

### Superscripts

-	average
---	---------

## REFERENCES

1. Almengor JG, Penuela G, Wiggins ML, Brown RL, Civan F, & Hughes RG (2002), User's Guide and Documentation Manual For BOAST-NFR For Excel. (DE-AC26-99BC15212), Norman, Oklahoma, USA.
2. Barenblatt, G. I., Zeltov, I. P., & Kochina, I. N. (1960), Basic Concepts in the Theory of Seepage of Homogeneous Liquids in Fissured Rocks. *Journal of Applied Mathematical Mechanics* **24**(5), 1286-1303.
3. Coats KH (1989), Implicit Compositional Simulation of Single-Porosity and Dual-Porosity Reservoirs. Paper SPE 18427 presented at the *SPE Symposium on Reservoir Simulation*, Houston, Texas, USA, 6-8 February.
4. Chang MM (1993), Deriving the Shape Factor of a Fractured Rock Matrix. *Technical Report NIPER-696 (DE93000170)*, NIPER, Bartlesville, Oklahoma, USA.
5. Dutra Jr., T. V., & Aziz, K. (1992), A New Double-Porosity Reservoir Model for Oil/Water Flow Problems. *SPE Journal* **7**(4), 419-425.
6. Firoozabadi A & Thomas LK (1990), Sixth SPE Comparative Solution Project: Dual-Porosity Simulators. *Journal of Petroleum Technology* **42**(6), 710-715, 762-763.
7. Heinemann ZE & Mittermeir GM (2012), Derivation of the Kazemi–Gilman–Elsharkawy Generalized Dual Porosity Shape Factor. *Transport in Porous Media* **91**(1), 123-132.
8. Kazemi, H. (1969), Pressure Transient Analysis of Naturally Fractured Reservoirs With Uniform Fracture Distribution. *SPE Journal* **9**(4), 451-462.
9. Kazemi H, Merrill LS, Porterfield KL, & Zeman PR (1976), Numerical Simulation of Water-Oil Flow in Naturally Fractured Reservoirs. *SPE Journal* **16**(6), 317-326.
10. Kazemi H & Gilman JR (1992), Analytical and Numerical Solution of Oil Recovery From Fractured Reservoirs With Empirical Transfer Functions. *SPE Reservoir Engineering* **7**(2), 219-227.

11. Lim KT & Aziz K (1995), Matrix–Fracture Transfer Shape Factors for Dual-Porosity Simulators. *Journal of Petroleum Science and Engineering* **13**(3-4), 169–178.
12. Lough, M. F., Lee, S. H., & Kamath, J. (1997), A New Method To Calculate Effective Permeability of Gridblocks Used in the Simulation of Naturally Fractured Reservoirs. *SPE Reservoir Engineering* **12**(3), 219-224.
13. Lu, H., Donato, G. D., & Blunt, M. J. (2008), General Transfer Functions for Multiphase Flow in Fractured Reservoirs. *SPE Journal* **13**(3), 289-297.
14. Penuela G (2002), Modeling Interporosity Flow for Improved Simulation of Naturally Fractured Reservoirs. Ph.D. Dissertation, Oklahoma University, Norman, Oklahoma.
15. Penuela G, Civan F, Hughes RG, & Wiggins ML (2002), Time-Dependent Shape Factors for Secondary Recovery in Naturally Fractured Reservoirs. Paper SPE 75234 presented at the *SPE/DOE Improved Oil Recovery Symposium, Tulsa, Oklahoma*, 13-17 April 2002.
16. Penuela G, Civan F, Hughes RG, & Wiggins ML (2002), Time-Dependent Shape Factors for Interporosity Flow in Naturally Fractured Gas-Condensate Reservoirs. Paper SPE 75524 presented at the *SPE Gas Technology Symposium, Calgary, Alberta, Canada*, 30April-2May 2002.
17. Quintard M & Whitaker S (1995), Transport in Chemically and Mechanically Heterogeneous Porous Media. II: Comparison with Numerical Experiments for Slightly Compressible Single-phase Flow. *Advances in Water Resources* **19**(1), 49-60.
18. Rangel-German ER (2002), Water Infiltration in Fractured Porous Media: In-situ Imaging, Analytical Model, and Numerical Study. Ph.D. Dissertation, Stanford University, Stanford, California.
19. Rangel-German ER & Kovscek AR (2005) Matrix-Fracture Shape Factors and Multiphase-Flow Properties of Fractured Porous Media. Paper SPE 95105 presented at the *SPE Latin American and Caribbean Petroleum Engineering Conference, Rio de Janeiro, Brazil*, 20-23 June 2005.
20. Sarda S, Jeannin L, Basquet R, & Bourbiaux B (2002) Hydraulic Characterization of Fractured Reservoirs: Simulation on Discrete Fracture Models. *SPE Reservoir Evaluation & Engineering* **5**(2), 154-162.

21. Sarma P (2003) New Transfer Functions for Simulation of Naturally Fractured Reservoirs with Dual Porosity Models, Ph.D. Dissertation, Stanford University, Stanford, California.
22. Sarma P & Aziz K (2006) New Transfer Functions for Simulation of Naturally Fractured Reservoirs With Dual-Porosity Models. *SPE Journal* **11**(3), 328-340.
23. Ueda Y, Murata S, Watanabe Y, & Funatsu K (1989) Investigation of the Shape Factor Used in the Dual-Porosity Reservoir Simulator. Paper SPE 19469 presented at the *SPE Asia-Pacific Conference*, Sydney, Australia, 13-15 September.
24. Warren JE & Root PJ (1963) The Behaviour of Naturally Fractured Reservoirs. *SPE Journal* **3**(3), 245-255.
25. Zhang X, Hu Y, Fan R, Baozhu, Li, & Zhang S (2010) Comparison of Oil Displacement by Water Between Naturally Fractured Reservoir and Vuggy Fractured Reservoir Based on Streamline Technique. Paper SPE 131075 presented at the *CPS/SPE International Oil & Gas Conference and Exhibition*, Beijing, China, 8–10 June.

## APPENDIX

### A.1. Visualization of reservoir problem (shape factor comparison)

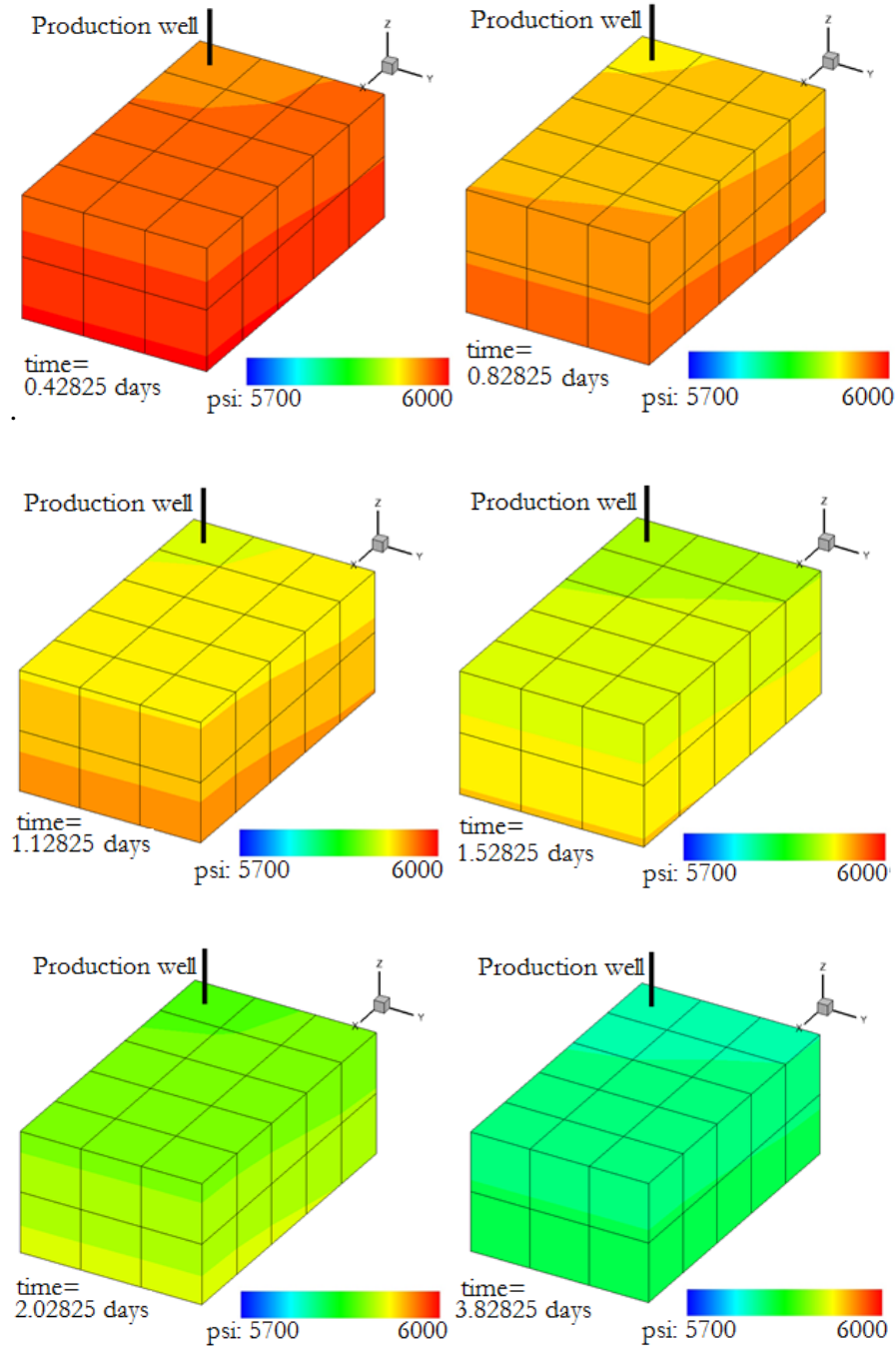


Figure 18: One of the simulations runs using Kazemi's shape factor for tetrahedron.

This simulation shows the pressure profile throughout the matrix blocks. Simulator codes were modified to be able to generate results for the purpose of visualization. It

was observed that the pressure profiles are decreasing for the matrix blocks that are nearer to the production well. Fluid flows always happen in the direction from high pressure into low pressure area. The pressure profiles indicate that flow are towards to the direction of well.

The purposes of having this visualization are to:

- a. The visualization was important to reconfirm whether the simulation results are reasonable.
- b. Visualization is an effective method to describe simulation results. Additionally, it can provide a better understanding about reservoir simulation.

## A.2. Derivation of correlation of transfer rate and $P_d / t_d$

Eq. (2.20) can be differentiated with time to obtain Eq. (A1)

$$\frac{\partial}{\partial t} \left( \frac{\bar{p}_m - p_i}{p_f - p_i} \right) = \frac{\pi^2}{\phi \mu c_t} \left( \frac{k_x}{L_x^2} + \frac{k_y}{L_y^2} + \frac{k_z}{L_z^2} \right) \left( \frac{p_f - \bar{p}_m}{p_f - p_i} \right) \quad (\text{A1})$$

By using finite approximations for first degree derivative, Eq. (A1) can be rewritten as Eq. (A2).

$$\frac{\left( \frac{\bar{p}_m - p_i}{p_f - p_i} \right)_2 - \left( \frac{\bar{p}_m - p_i}{p_f - p_i} \right)_1}{\Delta t} = \frac{\pi^2}{\phi \mu c_t} \left( \frac{k}{L^2} \right) \left( \frac{p_f - \bar{p}_m}{p_f - p_i} \right) \quad (\text{A2})$$

For sufficient small points, and if  $p_f = \text{constant}$ , then

$$\frac{(\bar{p}_m)_2 - (\bar{p}_m)_1}{\Delta t} = \frac{\pi^2}{\phi \mu c_t} \left( \frac{k}{L^2} \right) (p_f - \bar{p}_m) \quad (\text{A3})$$

Substitute Eq. (A3) into the given Eq. (A4), we get Eq. (A5).

$$\tau_{mf} = -\rho \phi c_t \frac{\partial \bar{p}_m}{\partial t} \quad (\text{A4})$$



$$\tau_{mf} = \frac{-\rho\pi^2}{\mu} \left( \frac{k}{L^2} \right) (p_f - \bar{p}_m) \quad (\text{A5})$$

if  $\left( \frac{k}{\phi\mu c_i L^2} \right)$  = equivalent, while t varies, then Eq. (A2) can be rewrite into Eq. (A6).

$$\frac{\left( \frac{\bar{p}_m - p_i}{p_f - p_i} \right)_2 - \left( \frac{\bar{p}_m - p_i}{p_f - p_i} \right)_1}{\left( \frac{kt}{\phi\mu c_i L^2} \right)_2 - \left( \frac{kt}{\phi\mu c_i L^2} \right)_1} \times \frac{1}{\pi^2} \times (p_f - p_i) = (p_f - \bar{p}_m) \quad (\text{A6})$$

Substitute Eq. (A6) into Eq. (A5), we get Eq. (A7).

$$\tau_{mf} = \frac{\left( \frac{\bar{p}_m - p_i}{p_f - p_i} \right)_2 - \left( \frac{\bar{p}_m - p_i}{p_f - p_i} \right)_1}{\left( \frac{kt}{\phi\mu c_i L^2} \right)_2 - \left( \frac{kt}{\phi\mu c_i L^2} \right)_1} \times \frac{\rho k}{\mu L^2} \times (p_i - p_f) \quad (\text{A7})$$

$$\tau_{mf} = \frac{\partial p_d}{\partial t_d} \left( \frac{\rho k}{\mu L^2} (p_i - p_f) \right) \quad (\text{A8})$$

### A.3. Water saturation profile in reservoir blocks using various transfer functions

The Figure A2- Figure AX shows the water saturation profile in reservoir matrix blocks and fractures blocks. Notice that there are some differences in water propagation in the reservoir blocks. The simulation showed that water propagation using transfer function from Rangel-German & Kovscek (2005) is the slowest, followed by Sarma & Aziz (2006), and Warren & Root (1963). Both German & Kovscek (2005) and Sarma & Aziz (2006) have additional imbibition terms to account for the additional matrix-fracture transfer rate.

### A.3.1 Simulation using Warren & Root (1963) transfer function

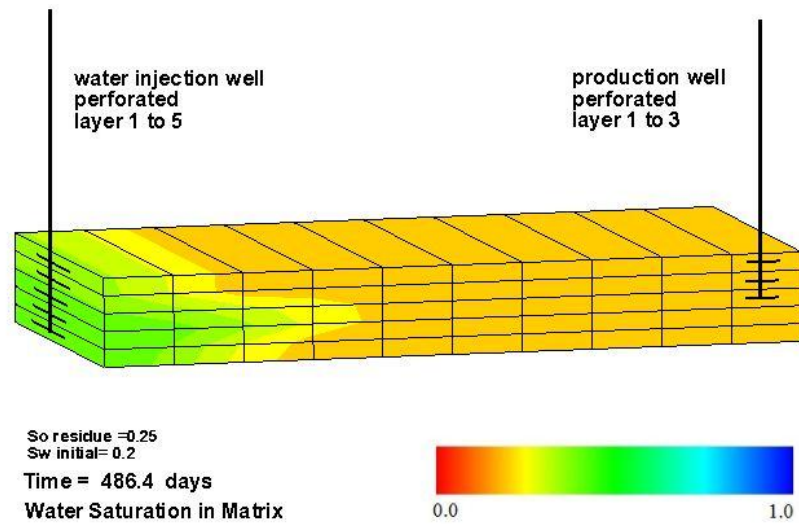


Figure 19: Water saturation in matrix blocks at time=486.4days

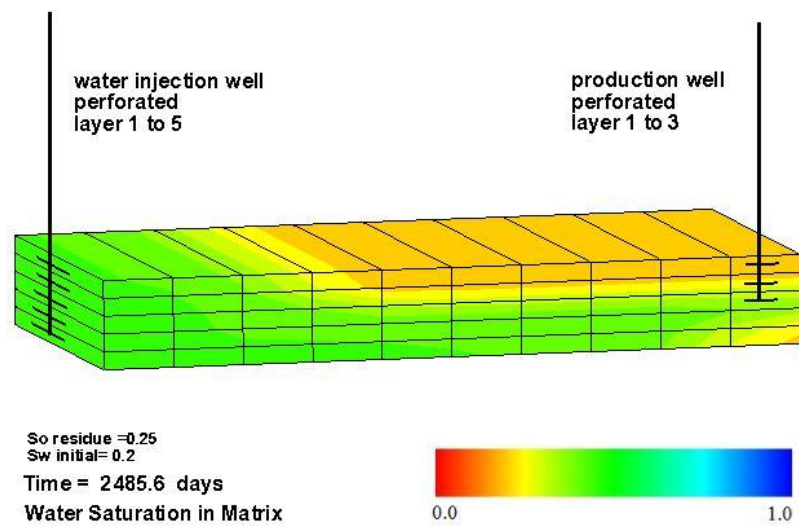


Figure 20: Water saturation in matrix blocks at time=2485.6days

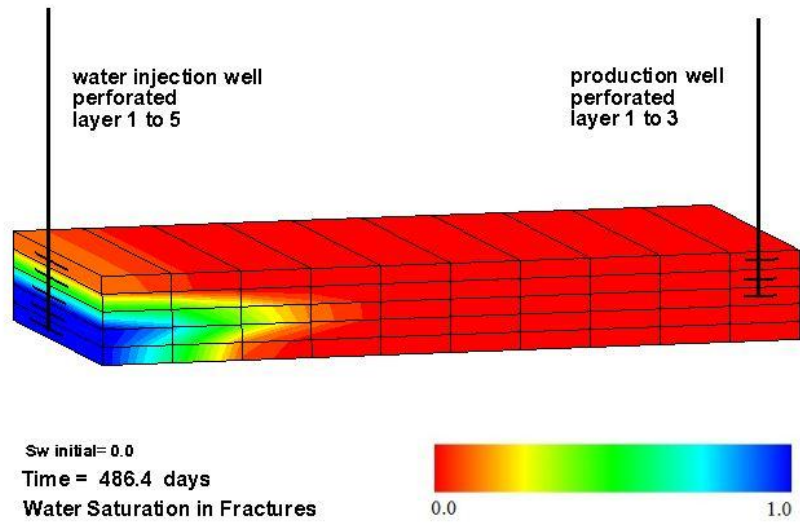


Figure 21: Water saturation in fractures at time=486.4days

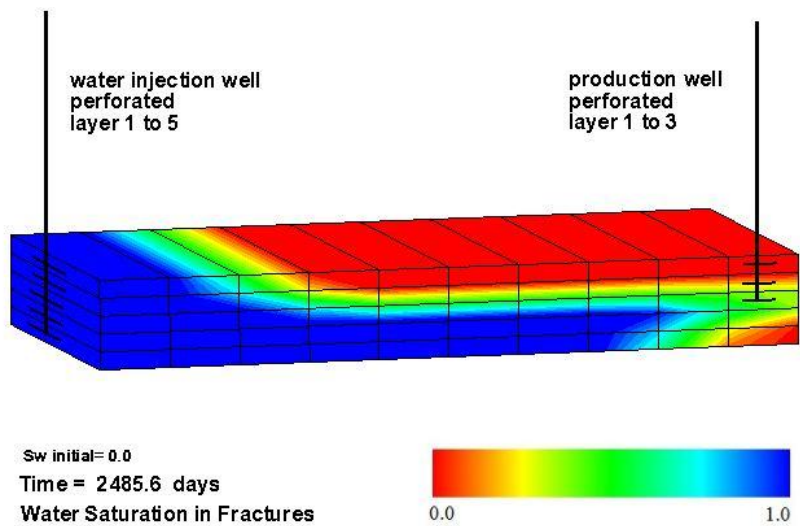


Figure 22: Water saturation in fractures at time=2485.6days

### A.3.2 Simulation using Sarma & Aziz (2006) transfer function

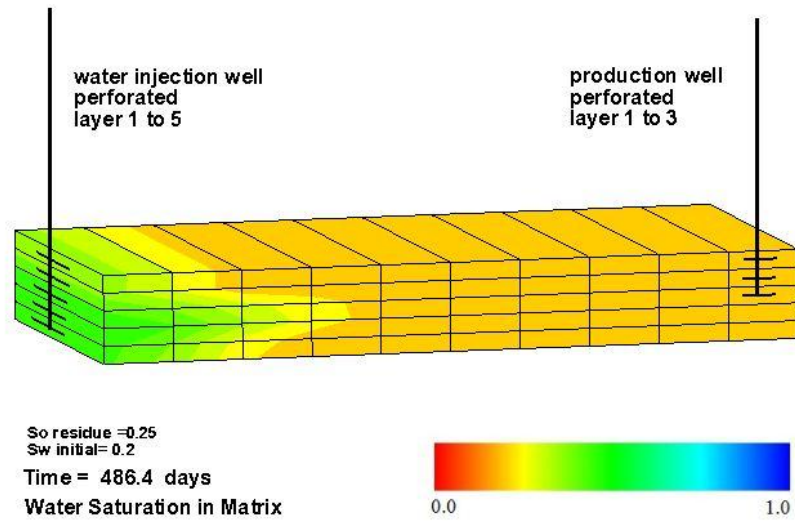


Figure 23: Water saturation in matrix blocks at time=486.4days

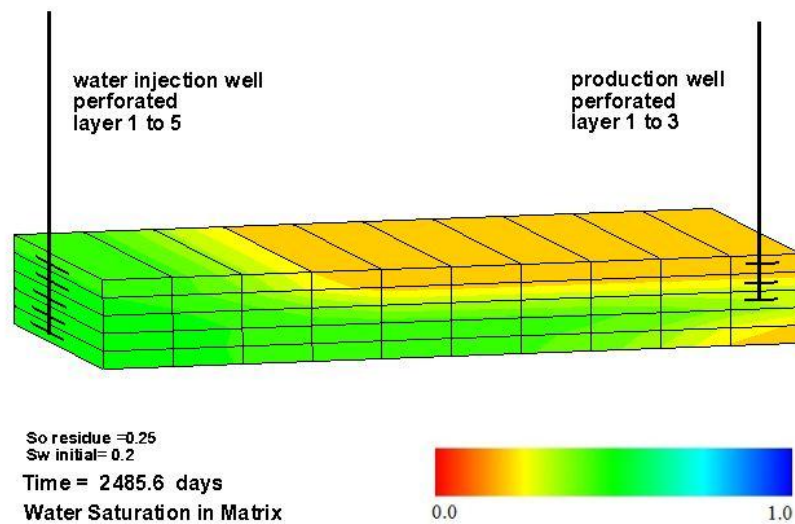


Figure 24: Water saturation in matrix blocks at time=2485.6days

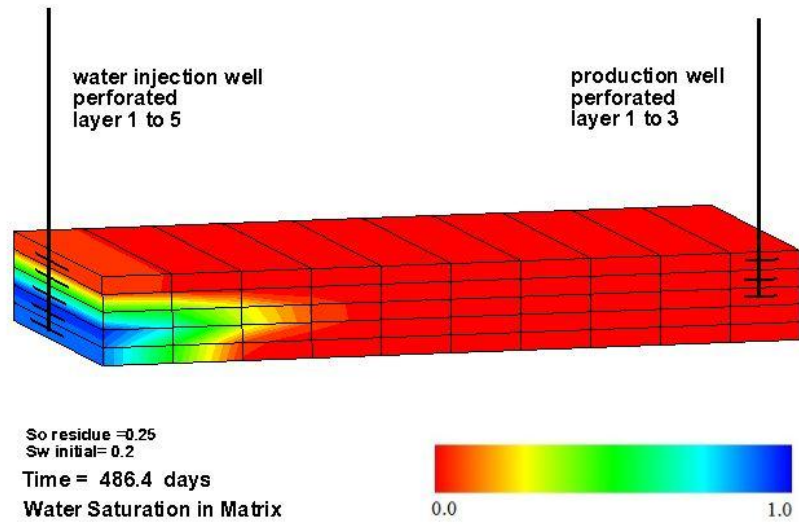


Figure 25: Water saturation in fractures at time=486.4days

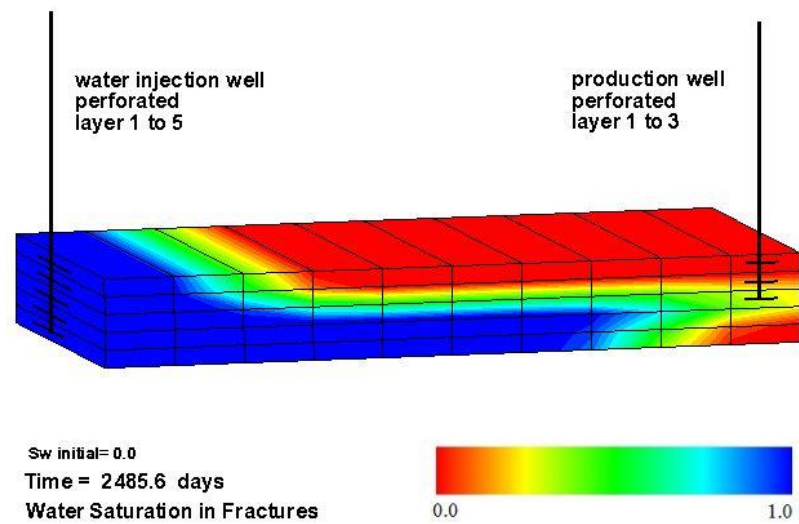


Figure 26: Water saturation in fractures at time=2485.6days

### A.3.3 Simulation using Rangel-German & Kovscek (2005) transfer function

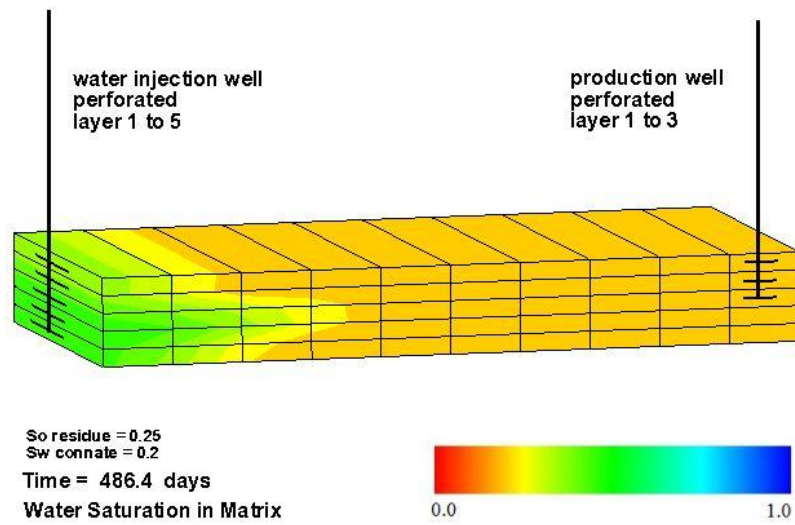


Figure 27: Water saturation in matrix blocks at time=486.4days

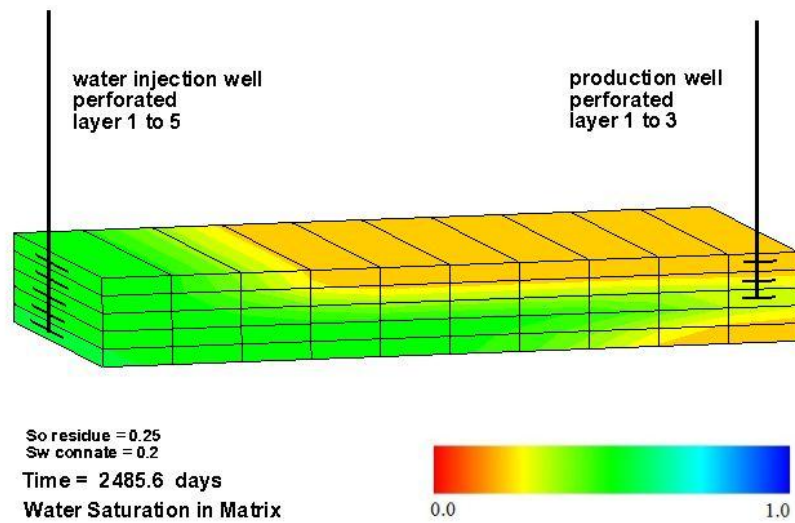


Figure 28: Water saturation in matrix blocks at time=2485.6days

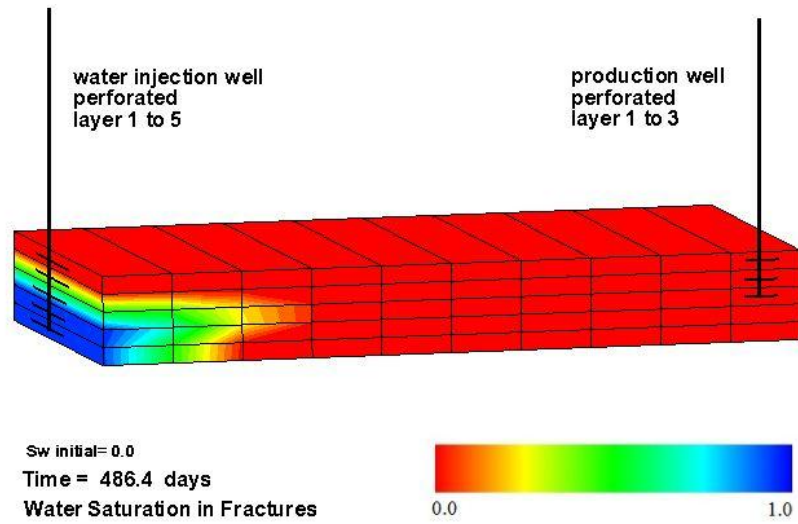


Figure 29: Water saturation in fractures at time=486.4days

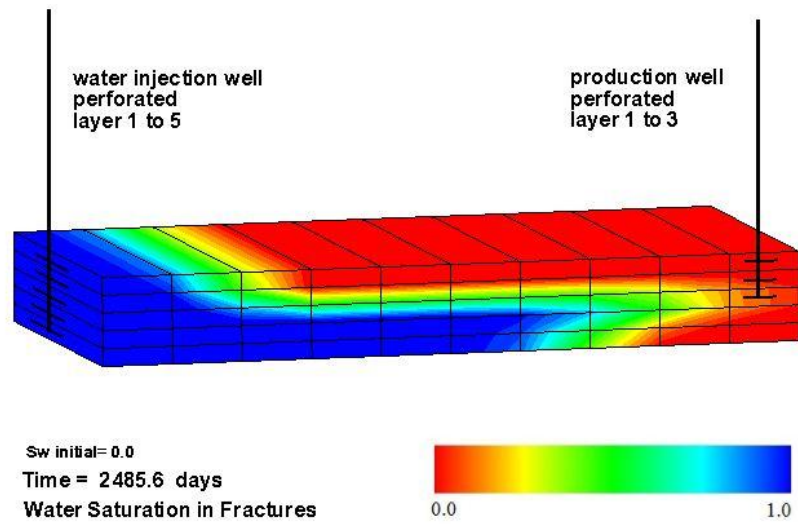


Figure 30: Water saturation in fractures at time=2485.6days